

Received November 30, 2020, accepted December 13, 2020, date of publication December 30, 2020,  
date of current version January 12, 2021.

Digital Object Identifier 10.1109/ACCESS.2020.3048148

# Adaptive Entropy Index Histogram Equalization for Poor Contrast Images

SAMER HAMEED MAJEED<sup>ID</sup> AND NOR ASHIDI MAT ISA<sup>ID</sup>, (Member, IEEE)

School of Electrical and Electronic Engineering, Engineering Campus, Universiti Sains Malaysia, Penang 14300, Malaysia

Corresponding author: Nor Ashidi Mat Isa (ashidi@usm.my)

This work was supported by the Universiti Sains Malaysia Research University Individual (RUI) Grant, entitled 'Development of Automatic Intelligent Karyotyping System of Classifying Abnormal Chromosome' with account number 1001/PELECT/8014030.

**ABSTRACT** Hidden details and lack of image contrast can be attributed to limited user experience, poor device quality, environment settings during image acquisition, and illumination. To address these problems, techniques based on histogram equalization (HE) have been frequently used to reduce these problems and to improve image contrast. However, the resultant images obtained by techniques often appear unnatural possibly due to washed-out effects and unwanted artifacts. This study proposes a new technique called adaptive entropy index histogram equalization (AEIHE) that belongs to the local sub-class of HE-based contrast enhancement techniques. AEIHE initially divides the image into three sub-images to enhance and highlight its local details. Each of these sub-images uses a different contextual region and clip limit based on the richness of their information and their structure, both of which are adaptively determined by AEIHE. A new parameter called Entropy-Index is then used to ensure the high information richness of the resultant sub-image while preserving its structure. AEIHE guarantees the production of an excellent resultant image by combining enhanced sub-images. Quantitative evaluations of 819 images show that AEIHE has successfully produced excellent resultant images with improved contrast, highlighted local details, and minimized effects of artifacts and unwanted noise. Therefore, AEIHE has a high application potential in the medical imaging, machine vision, and industrial domains.

**INDEX TERMS** Histogram equalization-based technique, histogram entropy, histogram clip limit, window size.

## I. INTRODUCTION

Many image capturing devices, such as mobile phones, digital cameras, and security cameras, have been developed over the past decades and are commonly used by humans for personal, documentary, satellite, medical, and scientific use. However, the quality of images captured by these devices remains subjective and depends on several factors, such as illumination, user experience, and quality of camera lenses. In this case, poor illumination, contrast, and noise in image can all affect image quality. Therefore, image enhancement plays a crucial role in image processing, a process that involves image segmentation, features extraction, and image type classification, among others. Image segmentation preserves the important regions in an image and extracts homogeneous regions that contain few objects, such as the sky, sea, and wall [1]. Improvement techniques are thus designed

The associate editor coordinating the review of this manuscript and approving it for publication was Rajeswari Sundararajan.

to achieve optimum conditions and to obtain images with excellent visuality by enhancing their contrast or maintaining their brightness [2].

Contrast improvement is important in image quality assessment and has been widely applied in medical, satellite, and military images, among others [3]. The intensity of pixels in an image is modified by using contrast enhancement techniques, and the imparity between the foreground and background regions is increased in the process [4]. The techniques used for improving image contrast can be classified into (i) frequency and (ii) spatial domains [3]. Those techniques in the frequency domain enhance the image in three steps, namely, (i) by calculating the Fourier transform of the original image, (ii) manipulating the transform coefficients, and (iii) applying inverse Fourier transform to produce the resultant image. The transform coefficients are manipulated by using either discrete cosine transforms (DCTs) or the discrete wavelet transforms (DWTs) [5]. The advantages of using frequency domain techniques lie in their capability to

reduce the computational time and preserve the frequency composition of the original image. However, these techniques also have the following disadvantages: (i) they are purely subjective because during the enhancement process, determining the values of optimum parameters greatly depends on user experience, and (ii) they are incapable of simultaneously enhancing all regions of an image [5]. Meanwhile, many techniques in the spatial domain have been developed, including: (i) histogram equalization (HE), (ii) gray-level grouping, and (iii) unsharp masking [5], [6].

#### A. HISTOGRAM EQUALIZATION

Histogram equalization (HE) technique, an image enhancement technique in the spatial domain, HE operates and manipulates the pixel intensity of images directly without converting them to another domain (i.e., frequency domain). The HE technique redistributes the image intensity evenly across the entire range of the gray levels to enhance the image contrast. The intensities are redistributed by (i) combining multiple gray levels with few probabilistic densities into a single gray level, and (ii) increasing the gap between two gray-level neighbors with high density. This technique has two sub-classes, namely, (i) conventional histogram equalization (CHE) and (ii) hybrid histogram equalization [7]. The CHE sub-class is further subdivided into (i) global histogram equalization (GHE), (ii) bi-sub-imaging histogram equalization (BSHE), (iii) multi-sub-imaging histogram equalization (MSHE), (iv) weighted histogram equalization (WHE), (v) local histogram equalization (LHE), and (vi) exposure region histogram equalization (ERHE).

##### 1) GLOBAL HISTOGRAM EQUALIZATION

GHE is the first sub-class of CHE, it increases the contrast of an entire image. This simple, effective enhancement technique [8] redistributes the bins density and extends the gray-level dynamic range to enhance the image contrast in comprehensive mode [8]. Moreover, GHE uses the cumulative density function (CDF) of an image as its basic level for contrast enhancement [8]. This technique is frequently used in tracking, and real-time applications due to its simplicity, efficiency, and processing time [3]. Nevertheless, the resultant images are washed out due to the shifting effect of the original image mean value [9], [10]. Moreover, GHE technique is unable to retain the information of the original image due to the high-frequency concentration at certain gray levels that predominate at the other low-frequency levels, such as small regions and the background. These disadvantages generate contradictory limits at certain levels and detailed losses at other low levels [11]. Dynamic clipped histogram equalization (DCLHE) is a technique used in the GHE sub-class that improves images with poor contrast [12]. This technique initially eliminates the zero density of intensity levels from the image histogram. Afterward, the non-zero density gray levels are clipped with a minimal histogram value. Finally, CHE is eventually applied to enhance contrast. According to [12], DCLHE can maintain the entropy of an image and produce

a uniform distribution of the gray level. However, DCLHE cannot maintain image brightness and is only effective for a limited range of histogram gray levels.

##### 2) BI SUB-IMAGING HISTOGRAM EQUALIZATION

BSHE is the second sub-class of CHE that overcomes the disadvantage of GHE in preserving illumination by creating two sub-histograms from the original image histogram. Various versions of BSHE, including brightness-preserving bi-histogram equalization (BBHE) [13], dual sub-image HE (DSIHE) [14], minimal mean brightness error bi-histogram equalization (MMBEBHE) [15], Otsu-based BBHE bi-histogram equalization (OBHBE) [16], entropy-based bi-histogram equalization (EBBHE) [16], bi-histogram-equalization-based three plateau limits (BHE3PL) [17], and range-limited bi-histogram equalization (RLBHE), have been developed [18]. BBHE and DSIHE retain image brightness by creating two sub-histograms based on the mean and median values of the original histogram, respectively. MMBEBHE technique explores a threshold value that acquires the minimum brightness error (MBE) to divide the image histogram. Similar to GHE, these techniques suffer from high-frequency dominance if the sub-histogram contains several dominant levels that may produce a resultant image with unwanted noise that cannot be maintained [12], [19]. MMBEBHE also suffers from a long processing time [19]. OBHBE and EBBHE use Otsu and entropy based on the histogram threshold of an image. The resulting images from these techniques are superior over those produced by BBHE, DSIHE, and MMBEBHE given their ability to preserve image brightness. However, these techniques suffer from an inefficient improvement in image contrast [20]. According to [17], BHE3PL can produce an excellent resultant image with superior image quality. As another technique that uses Otsu, RLBHE [18] divides the histogram of an image into two sub-histograms, separates the background from the foreground, and preserves the image brightness. However, RLBHE washes out the image details [21].

##### 3) MULTI SUB-IMAGING HISTOGRAM EQUALIZATION

The MSHE is the third sub-class of CHE that can be further subdivided into recursive mean separate histogram equalization (RMSHE) [22], recursive sub-image histogram equalization (RSIHE) [23], median-mean-sub-image based clipped histogram equalization (MMSICHE) [24], and adaptive thresholding-based sub-histogram equalization (ATSHE) [25]. Similar to DSIHE, RMSHE and RSIHE use the mean and median values as their thresholds, respectively, but in recursive mode and are able to preserve image brightness through multiple decompositions. However, the repeating decomposition process of these techniques extends the processing time and amplifies noise due to the manual selection of the recursive level ( $r$ ) based on visual judgement. If the  $r$ -level is substantially high, then only negligible improvements in the image will be observed. Similar

to BBHE, MMSICHE computes the mean value to create four sub-histograms of the original histogram by setting the value of 2 to the recursive level. Afterward, similar to DSIHE, MMSICHE computes the median value to clip each sub-histogram. CHE is then applied on these sub-histograms. Meanwhile, ATSHE initially computes the peak signal-to-noise ratio (PSNR) value to count the number of sub-histograms at each stage and then uses the standard deviations and mean values to obtain the thresholds. ATSHE then uses the median value of the histogram to clip and enhance the image contrast. While this technique can preserve the brightness of images with poor illumination, ATSHE suffers from the following limitations: (i) manually counting the amount of iterations extends the processing time and results in negligible improvements; (ii) certain regions of the image are washed out, thereby resulting in ambiguous details; and (iii) this technique has only been tested on a limited number of images.

Dynamic histogram equalization (DHE) [26] and brightness preserving dynamic histogram equalization (BPDHE) [9] have been proposed to prevent histogram compression, washout, and other notable over-enhancement problems. DHE divides the histogram of the original image into multiple sub-histograms depending on the local minima value until no dominant segment is observed in any of these sub-histograms. However, the image produced by this technique suffers from an overbrightness problem despite comprehensively maintaining the image details [9]. Meanwhile, BPDHE divides the image histogram by using the local maximum and Gaussian filter. While this technique effectively addresses the excessive brightness produced by DHE, BPDHE also creates sub-histograms of different ranges. Few of these sub-histograms show limited gray-level ranges, whereas the other sub-histograms have large gray-level ranges. Several sub-histogram ranges can lead to a non-uniform improvement in an image [9].

Quadrants for dynamic histogram equalization (QDHE) [27] technique has been proposed to retain over-enhancements in contrast and noise amplification and produces an image with detailed preservation. After dividing the histogram into several sub-histograms, QDHE computes for the mean value of each sub-histogram to adjust the clipping value. A new dynamic range is then formed by using the DHE feature from the resultant sub-histograms. Meanwhile, adaptively raising the value of histogram equalization HE (AIVHE) [28] prohibits serious changes in the PDF image by redistributing the original PDF. However, one downside of AIVHE lies in its parameter specification, which requires manual human intervention [28]. By contrast, entropy-based dynamic sub-histogram equalization (EDSHE) [29] was proposed to address the drawbacks of RMSHE by measuring the entropy value for each recursive layer and then comparing this value with the initial value. Unfortunately, EDSHE produces uncounted artifacts in the resultant image and requires a longer processing time compared with CHE and RMSHE.

#### 4) WEIGHTED HISTOGRAM EQUALIZATION

WHE techniques modify the image histogram to regulate the improvement rate of the dominant gray level. These techniques may preserve the image details by transforming or clipping the histogram levels and eliminating the dominance of high-frequency histogram levels.

Dominant gray levels have lesser weight than the original histogram after the modification stage, thereby resulting in minimal improvements in the resultant image captured by WHE compared with those obtained by the three aforementioned CHE sub-classes. The contrast enhancement techniques developed under WHE include modified histogram equalization for contrast enhancement (MHE) [11], weighted threshold histogram equalization (WTHE) [30], recursively separated and weighted histogram equalization for brightness preservation and contrast enhancement (RSWHE) [31], range limited weighted histogram equalization (RLWHE) [4], edge preservation local histogram equalization (EPLHE) [32], a logarithmic law-based histogram modification scheme for naturalness image contrast enhancement [33], a bi-histogram modification method for images with non-uniform illumination and low contrast [34], image enhancement via sub-image histogram equalization based on mean and variance (MVSIE) [19], weighted average multi-segment histogram equalization (WAMSHE) [35], and High Speed Quantile Based Histogram Equalization for Brightness Preservation and Contrast Enhancement (HSQHE) [36].

MHE is designed to prevent the formation of artifacts in RMSHE, DSIHE, and BBHE and to improve the appearance of the resultant image. This technique alters the histogram of the original image and then applies CHE to enhance contrast. However, MHE has the following disadvantages: (i) obtaining the optimal parameter value is highly subjective, thereby complicating the achievement of the optimum improvement result; and (ii) reducing the high-frequency histogram level can lead to loss of information. WTHE modifies the PDF values of the original image and then applies CHE on the modified PDF. This technique can also be adapted to the over-enhancement process. Despite its high speed, WTHE is unable to maintain the brightness of the image, which in some cases produces unwanted artifacts.

RSWHE is divided into RSWHE-M and RSWHE-D where RSWHE-M computes the mean value to divide the histogram similar to RMSHE but in recursive mode, whereas the latter the RSWHE-D divides the histogram by using the same median value as the RSIHE but in recursive mode. These sub-histograms are then altered by using a normalized power-law distribution function. Afterward, conventional HE is applied to all sub-histograms. RSWHE-M and RSWHE-D achieve a remarkable brightness conservation and a considerable improvement in contrast, but the resultant image contains unwanted artifacts due to the loss of several image details [4], [12], [28]. In addition, RLWHE is designed to control contrast improvement and maintain image brightness. This technique is quick and can be used

in real-time applications. To reduce intra-class variance, two sub-histograms are created from the original image histogram. The PDF is then weighted and modified for each sub-histogram, and CHE is used to limit the brightness of each sub-histogram. Adaptive gamma correction is then applied to improve the information richness of the image and prevent the introduction of unwanted artifacts. At the last processing stage, a homographic filter is used to reduce the effects of artifacts. The of EPLHE argued that partially over-loaded sub-imaging HE (POSHE) cannot retain the edges of the image objects; in case that the sub-image is a member of zero-textured regions. Then the information richness of that region would be minimal, and the CDF values would demonstrate inadequate changes, which could lead to over- and/or under-enhancement problems [32]. The EPLHE technique solves the improvement issue by dividing the original image into non-overlapped and equally sub-images and then using SOBEL operator to calculate the proportion of gradients in sub-images. The SOBEL operator is a powerful tool for detecting the edge of the object. EPLHE then applies bilateral Bezier-curve-based histogram equalization (BBCHE) to control the enhancement quality and reduce the computation time [37]. In BBCHE, each sub-image should be subdivided into two regions (bright and dark regions), with each region having two control point sets per region. BBCHE generates a smooth CDF that enhances the dark region and slightly decreases the bright region and then produces a weight setting proportional to each sub-image gradient information. Afterward, BBCHE generates weights that are proportional to each sub-image gradient information. All CDFs are then combined by weight. The disadvantage of EPLHE is that the sub-imaging process varies according to the size of the input image. In this case, EPLHE still preserves brightness in dark regions, thereby resulting in unpreserved image details. Moreover, the quantitative parameters are insufficient to measure the quality of the resultant image and to evaluate the performance of EPLHE.

A logarithmic-law-based histogram modifying the technique for natural image contrast was proposed in order to retain the pleasant aspect of an image by modifying its histogram in two stages [33]. The first stage employs an additional-based method to solve the histogram pit problem, whereas the second stage uses a logarithmic-law-based approach to overcome the histogram spike problem [33]. Afterward, CHE is employed to improve the contrast of the entire image. A local fine-tuning of the image is eventually performed by using DCT. However, this technique is unable to preserve image brightness, which may create dark regions in an image [34]. The technique proposed in [33] has three stages. First, a Gaussian low-pass filter is applied to avoid noise amplification and to extract illumination from the image. Second, the resultant image is divided into bright and dark regions by using a median in the threshold calculation, and the histogram of both regions is altered. Specifically, the dark region is moved to the segmentation threshold to increase brightness, whereas the bright area is moved

to the maximum value between the mean to the medium to prevent insignificant resultant image appearances. Third, the histogram of each region is cut off to be updated and redistributed in accordance with the change function. While this technique can reduce noise amplification, preserve image details, and enhance image entropy value, the resultant image has some blurred parts and artifacts.

MVSIHE uses three adaptive thresholds based on mean and variance to divide the histogram of the original image into four segments. Each of these segments is then modified and equalized by using CHE. This technique combines the improved segments and then normalizes them to reduce interference and intensity saturation. MVSIHE also creates a resultant image without introducing its artifacts and retains its mean brightness. However, MVSIHE is unable to retain or highlight details in white regions (i.e., the fourth section of the histogram, which is unable to highlight hidden details) and has a long processing time. Another technique called WAMSHE divides the histogram of the image into multiple sub-histograms and then equalizes each sub-histogram [35]. This technique preserves the mean image brightness and reduces unwanted noise and artifacts. Moreover, the HSQHE technique divides the histogram of the image into equal number of sub-histograms by using the parameter quantile ( $q$ ). Then, each quantile will be normalized, modified and equalized individually. After that, the whole histogram is normalized then equalized and produce the resultant image. If the number of intensities in the quantile is less, then the local details and regions in this sub-histogram may produce an unwanted artifacts and distortion in the image. Furthermore, setting the optimum value of  $q$  is too subjective and requires a highly user experience.

## 5) LOCAL HISTOGRAM EQUALIZATION

LHE, as the fifth sub-class of CHE, was developed to overcome the limitations of GHE. LHE can be applied to modify and enhance small gray-level regions and maintain image details bypassing the overall pixels of an image. For example, an image of  $640 \times 480$  image pixels must be equalized with a histogram 307200 times. The techniques under this sub-class include adaptive histogram equalization (AHE) [8], contrast-limited adaptive histogram equalization (CLAHE) [38], POSHE [39], cascaded multistep binomial filtering histogram equalization (CMBFHE) [40], adaptive image enhancement method using contrast limitation based on multiple layers (BOHE) [41], and iterated adaptive entropy clip limit histogram equalization (IAECHE) [5]. The AHE technique addresses the non-uniform illumination drawback of GHE by handling all image pixels and generates an image with homogenous brightness [8]. However, this technique has a long computation time, amplifies noise, and produces an image with an unnatural appearance [39]. In some cases, CLAHE, POSHE, and CMBFHE also produce images with poor appearance and noise effects [42], [43]. POSHE also demonstrates minimal improvements in computing time [39].

The authors in [41] claimed that POSHE improves the local information and reduces image noise in multiple stages. POSHE applies fast BOHE to achieve multilayer improvements of different window sizes created by the original image. For fast BOHE windows, if the size of the original image is  $M \times N$ , then the possible window sizes are  $M/2 \times N/2$ ,  $M/4 \times N/4$ , and  $M/8 \times N/8$ . The noise in all windows is minimized by using a contrast-limited technique. Fast BOHE is then applied to achieve improvements in each window. Afterward, the output is divided into small regions, which are then used to maintain local details through the fusion process. This technique is subject to a few disadvantages, including its (i) long computational time, (ii) inability to preserve the structure of the original image, and (iii) failure to improve the brightness of the resultant image. IAECHE divides an image into multiple blocks and uses the peaks from the histogram of these blocks to calculate the clip limit value [5]. Additionally, IAECHE computes the clip limit in an adaptive and iterative process to obtain the best clip limit value. Afterward, the enhanced blocks are combined to produce the resultant image. However, IAECHE has two drawbacks, namely, (i) its long processing time, and (ii) its inability to guarantee the optimal clip limit value.

## 6) EXPOSURE REGION HISTOGRAM EQUALIZATION

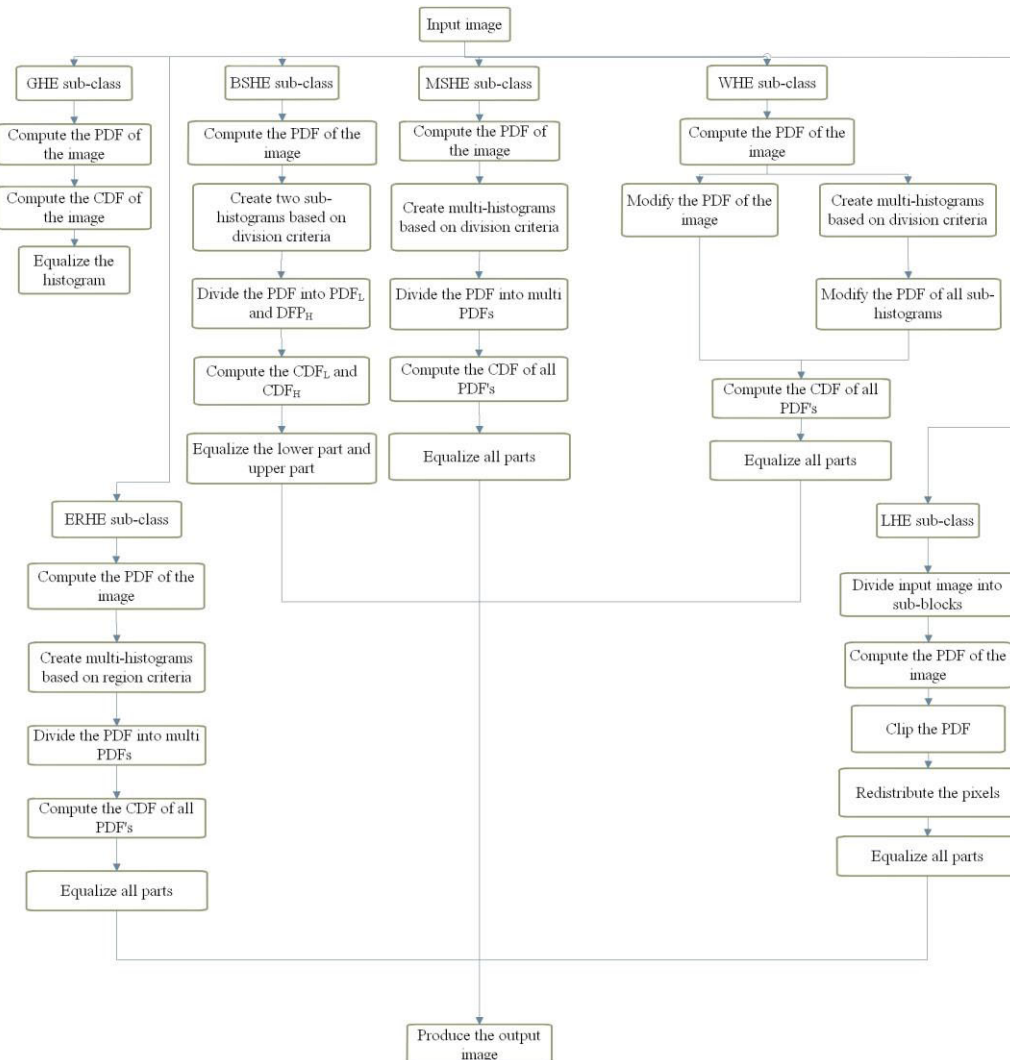
ERHE is the sixth CHE sub-class whose main concept is to divide the histogram into separate regions. ERHE aims to improve the illumination of images based on various regions and generate non-over-enhanced or under-enhanced output images. Some techniques that are used to maintain image brightness, especially for non-uniform illumination images, include exposure-based sub-image histogram equalization (ESIHE) [44], mean-based bi-histogram equalization plateau limit (mean-BHEPL) [45], median-based BHEPL (median-BHEPL) [45], adaptive bi-histogram equalization (ABHE) algorithm [45], and exposure-region-based multi-histogram equalization (ERMHE) [46].

The ESIHE technique uses an exposure threshold to divide the image histogram into two regions and then clips both of these sub-histograms with the mean gray level. These sub-histograms are then equalized by CHE. While this technique preserves image details and improves contrast, ESIHE does not work properly with images comprising several exposure regions. BHEPL and ABHE adapt to ESIHE by working with two areas of exposure (i.e., over- and under-exposure). However, these techniques do not operate in the normal exposure region. ERMHE addresses this multi-exposure region problem (i.e., over-, normal, and under-exposure) and produces an image with enhanced brightness protection and reduced noise. However, one region may be smaller than the other, and a high-density dominant problem is observed over low frequencies of gray levels, thereby causing information loss in some sections. The basic concept or approach of all CHE sub-class techniques is illustrated in Fig. 1.

## B. HYBRID HISTOGRAM EQUALIZATION

Solving real-world optimization problems is often considerably challenging, but many applications that deal with these problems are available. One main source of optimization algorithms is nature itself, which has inspired many researchers to obtain solutions to real-world problems. These algorithms are referred to as nature-inspired-based optimization algorithms (NIOA) [20]. In some cases, the obtained solution may not be the optimal one [47]. The important role of NIOA in computational intelligence, artificial intelligence, and machine learning has been recently proven [20]. HE-based image enhancement techniques have been expressed as optimization problems, and NIOAs have shown an efficient performance in addressing these problems.

The NIOAs algorithms can be classified into (i) evolution-, (ii) swarm-, (iii) physics-/chemistry-, and (iv) human-based algorithms. Those algorithms under the evolution-based category are based on the natural evolution of life. Some of these algorithms include the genetic algorithm (GA) [48], differential evolution (DE) [49], and genetic programming [50]. Meanwhile, those techniques under the swarm-based category are inspired by the social life and behavior of animal groups. These techniques include particle swarm optimization (PSO) [51], artificial bee colony (ABC) [52], ant colony optimization [53], firefly algorithm [54], and social spider optimization [55]. Those algorithms under the physics-/chemistry-based category are based on physics and chemistry laws and include simulated annealing [56] and gravitational search algorithm [57]. Human-based algorithms are based on human lifestyle, behavior, and social life and include harmony search [58] and imperialist competitive algorithm [59]. These optimization algorithms aim to maximize/minimize the fitness functions, such as by computing the entropy, PSNR, absolute mean brightness error (AMBE), energy, and contrast. Therefore, the fitness function is the main term for solving optimization problems. These algorithms also do not require specific information about the problem and are equipped with global and local search components to obtain optimal results. Given these features, NIOAs are efficient and powerful algorithms for solving problems in the image processing field, such as image enhancement, image segmentation, classification, and clustering. Several NIOAs have been hybridized with HE in the field of image enhancement to improve image contrast and preserve brightness such as [21], [60]–[67]. For instance, the authors in [60] hybridized PSO with CLAHE to enhance mammogram images. The objective function of PSO is to obtain the best entropy value and edge information. Meanwhile, the authors in [21] optimized the parameterized bi-thresholded HE by computing the entropy value in real-coded GA for brain magnetic resonance images (MRI). The authors in [61] hybridized the cuckoo search algorithm particle with OBBWTHE to obtain a quality index based on local variance and fractal dimension as multi-objective functions for mammogram images. The authors in [62] hybridized the ABC algorithm with MTHE to maximize entropy as the fitness

**FIGURE 1.** Illustrates the enhancement stages of the CHE sub-class.

function for histopathology images. The authors in [63] computed PSNR as an objective function to the firefly algorithm hybridized with OBBWTHE, EBBWTHE, and CLAHE for medical images. The authors in [64] maximized entropy by using PSO hybridized with gamma-correction-based HE for satellite images. The authors in [65] maximized entropy by hybridizing PSO with local-entropy-weighted HE for infrared images. The authors in [66] proposed a combination of the differential evolution and whale optimization algorithms to enhance image contrast. In this technique, the fitness function is treated as a combination of image entropy and image edge intensities. However, quantitative assessments were applied only on a limited number of images. The authors in [67] proposed a method based on the swarm of slaps folks that obtains the best fitness function by computing the percentage entropy of an image with other edge intensities and that of the PSNR of an image. They claimed that this method can produce an excellent image with a balanced contrast and

maintained brightness. However, this method suffers from the following drawbacks: (i) obtaining the optimum value takes up much time, and (ii) this method uses subjective parameters depending on user experience. Figure. 2 illustrates the HE- and the hybrid HE-based contrast enhancement techniques that have been proposed in the literature to address the limitations of these techniques.

Overall, there are several drawbacks to CHE and hybrid sub-classes. Specifically, the image produced by techniques under the GHE sub-class suffers from washout and loss of details. These techniques are therefore unsuitable for important applications, such as for medical and astronomical images. Meanwhile, techniques under the LHE sub-class require a long computational time, produce unwanted artifacts, and corrupt image brightness. The techniques under the BSHE and MSHE sub-classes suffer from a long computational time and face challenges in finding the optimal sub-imaging level. The techniques under the WHE

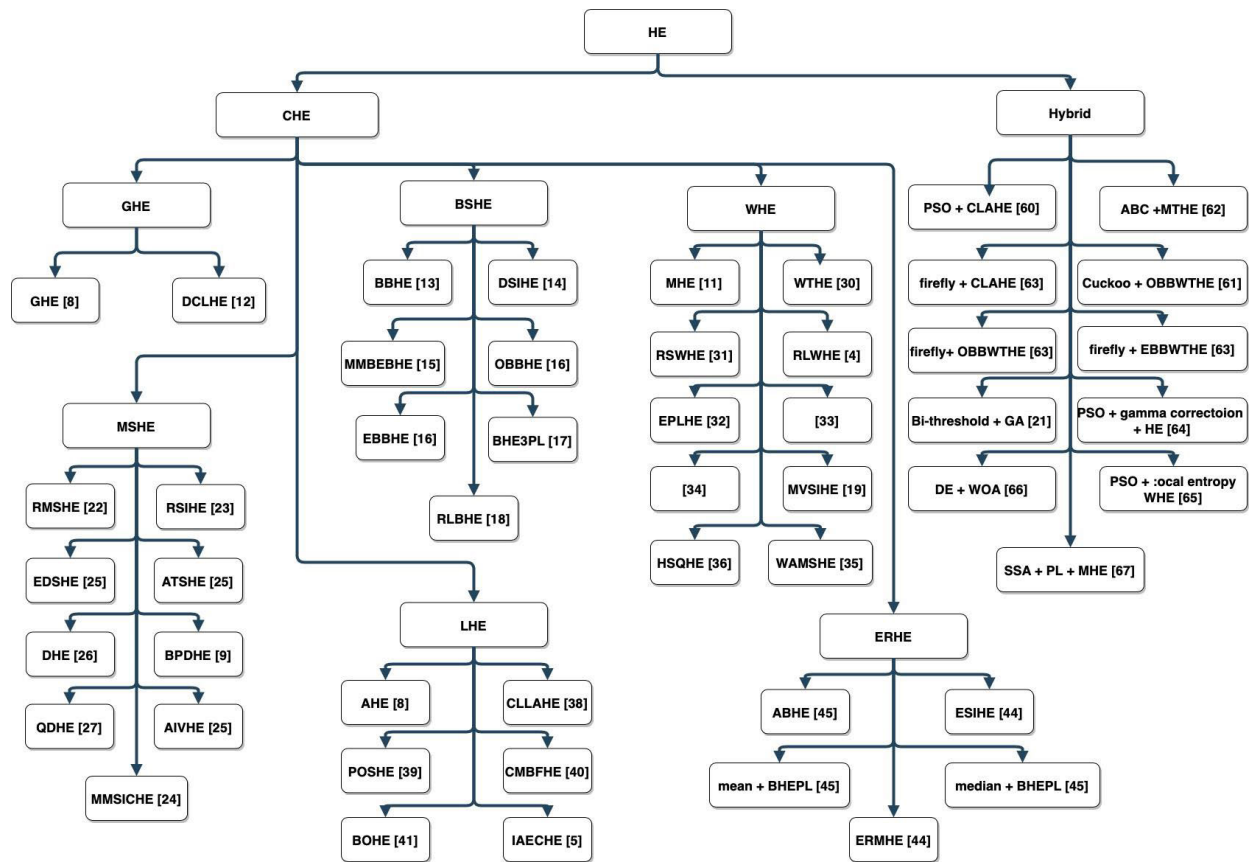


**FIGURE 2.** HE division and sub-classes.

sub-class are unable to preserve the image details and information in high-frequency dominant regions. The ERHE sub-class suffers from washed-out details in large spans, and the hybridized techniques with optimization algorithms suffer from long computational time and face difficulties in setting the optimum parameter values for computing the fitness function.

The abovementioned issues motivate this study to propose a new LHE technique for enhancing image contrast. The proposed technique aims to highlight the local details and enhance the information richness of the original image while preserving its structure. Despite belonging to the LHE sub-class, the proposed technique guarantees a uniform or even contrast distribution over the resultant image by adjusting all parameters adaptively and automatically. This objective contrast enhancement technique reduces the subjective effects of users while maintaining the image structure. In addition, a new approach for the local enhancement sub-class will be introduced to enhance the local image details without amplifying noise or producing unwanted artifacts.

Six quantitative assessments, namely, (i) AMBE, (ii) discrete entropy (DE), (iii) structure similarity index measurement (SSI), (iv) contrast improvement index (CII), (v) PSNR, (vi) and root mean square error (RMSE), are used to evaluate and compare the proposed technique with other

state-of-the-art techniques and to evaluate the quality of its resultant image.

## II. CONTRAST LIMITED ADAPTIVE HISTOGRAM EQUALIZATION

CLAHE is a LHE technique that was initially developed to improve low-contrast medical images [44]. This technique divides the original image into tiles or blocks that represent non-overlapping contextual areas. Two parameters, namely, clip limit (CL) and window size (WS), are used to control the degree of contrast enhancement and the quality of the resultant image. The brightness of the resultant image greatly depends on the CL value, where a large CL value will flatten the histogram of an image. By contrast, the dynamic gray level range increases along with decreasing WS, thereby reducing the image contrast. The original histogram is clipped for each contextual area, and the remaining pixels are redistributed over the entire gray-level range. Furthermore, the new histogram differs from the original one because the maximum intensity for all gray levels cannot exceed the CL value. Despite its advantages over GHE and AHE, CLAHE suffers from some significant drawbacks. First, CLAHE equally enhances the contrast of the background and foreground regions, thereby resulting in the high contrast of both regions in the resultant image. In other

words, CLAHE not only enhances the significant details of foreground regions but also the unimportant and unwanted details of the background regions. Poor resultant images may be produced when unwanted noises are present in the background regions. By enhancing these unwanted noises, unnatural and unpleasant resultant images may be produced as shown in Fig. 3.

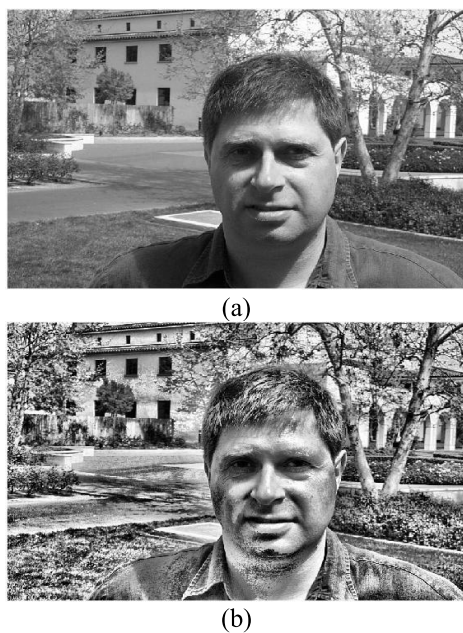


**FIGURE 3.** A noisy and unnatural image of CLAHE technique [5].

Second, the computation time in enhancing and producing the resultant image varies due to the differences in the size of the input image and the number of contextual regions, both of which are needed for the manipulation and enhancement of gray levels and for the preservation of details over the entire image. Figure 4 illustrates the time-consuming process of enhancing six different images using CLAHE. This illustration proves that various images require different computational times, with some images requiring only a few seconds to create the resultant image and others requiring a longer computational time.

Another drawback of CLAHE lies in its manual determination of WS and CL, which highly depends on the knowledge and experience of users. These users often refer to a general concept where a large CL can produce flat pixel distributions over the entire histogram, thereby producing noisy images, and a small CL barely improves the image contrast. Various images usually require different CL settings. Therefore, users should be familiar with both CLAHE and the original image features to produce the best resultant image. Table 1 shows the effect of setting various CL values in CLAHE [2]. Thus, the WS value also affects the natural look of the resultant image. Setting a small WS value generally leads to limited local image detail preservation with a low level of noise amplification, whereas a large value preserves the local

**TABLE 1.** Resultant PSNR using CLAHE technique with different clip limit value and block size of  $10 \times 10$ .

CL	PSNR
0.09	12.193
0.1	13.850
0.3	14.683
0.5	16.683

details but can amplify noise in the resultant image, thereby producing an unnatural resultant image. Table 2 presents the effects of various WS values [2]. Using the default values of CLAHE parameters may also lead to an over-enhanced contrast, which in turn will lead to the unpleasant appearance of the resultant image as shown in Fig. 5. Over-enhancement problems can be observed at many regions of the resultant image as shown in Fig. 5(b). Some over-enhanced regions are highlighted by blue squares in the figure. Therefore, choosing the optimum parameter value is crucial in enhancing image contrast by using CLAHE.

**TABLE 2.** Resultant PSNR using CLAHE technique with clip limit = 0.05 and various WS value.

WS	PSNR
$6 \times 6$	12.626
$8 \times 8$	12.966
$10 \times 10$	13.369

### III. PROPOSED ADAPTIVE ENTROPY INDEX HISTOGRAM EQUALIZATION METHODOLOGY

This study hypothesizes that obtaining a resultant image with good quality depends on the capability of an adaptive and automated strategy or approach to highlight information richness and details and to preserve the image structure. Accordingly, the proposed adaptive entropy index histogram equalization (AEIHE) technique aims to achieve the optimum entropy and optimum similarity index between the original and resultant image values. Achieving optimum entropy will enhance the information richness and details of an image, whereas obtaining the optimum similarity index will preserve the optimum image structure, thereby generating a good resultant image and controlling the over-enhancement problem faced by the conventional CLAHE.

To test this hypothesis, an image enhancement using AEIHE is performed in three stages, namely, (A) division of the original image into sub-images, (B) parameters initialization and optimization, and (C) construction of the resultant image. AEIHE introduces three new approaches to overcome the drawbacks of the conventional CLAHE and to produce a resultant image with clear local details, well-preserved



**FIGURE 4.** Processing time to produce resultant image by using conventional CLAHE technique (a) 0.8 second, (b) 2.35 seconds, (c) 1.64 second, (d) 3.26 seconds, (e) 1.86 second, (f) 3.26 seconds [5].

structure, and optimum contrast enhancement. These new approaches include the (i) adaptive calculation of the optimum clip limit ( $CL_{FACTOR}$ ), (ii) adaptive setting of the

optimum window size (WS), and (iii) introduction of a new image quality factor (i.e., *Entropy-Index*). The first two approaches are introduced to overcome the limitation of the



**FIGURE 5.** Example of resultant image produced by the CLAHE using the default parameters' values (a) Original image (b) the resultant image.

subjective process applied in the conventional CLAHE to obtain the optimum values for both parameters, whereas the *Entropy-index* is introduced as a fitness function to be fulfilled by AEIHE to realize the optimum image enhancement performance.

An image usually contains two main regions, namely, the foreground (or region of interest (ROI)) and the background. AEIHE assumes that an image can be divided into the left, center, and right regions (herein after referred to as left, center, and right sub-images).

The foreground regions or ROIs containing the most number of image details are assumed to be located at the center of the image, while the left and right sub-images refer to the background regions. Therefore, in the first stage, AEIHE divides the input image into these three sub-images.

In the second stage, the histogram of these sub-images is determined and used as an input to the whale optimization algorithm (WOA) [3] along with various WS values to obtain the optimum  $CL_{FACTOR}$  and WS. The WOA algorithm is a nature-inspired meta-heuristic optimization algorithm that mimics the social behavior of humpback whales to obtain the optimum solution to different problems by using the bubble-net hunting strategy (for additional information on the WOA algorithm, the reader can refer to [3]). The obtained optimum values for each sub-image are then applied to the conventional CLAHE to enhance the sub-images and to obtain the best

resultant sub-images. In the third stage, the three enhanced sub-images are combined to form the resultant enhanced image. Figs. 6 and 7 present the process design and the working flowchart of AEIHE, respectively. The following, sub-sections A, B, and C explain the first to third stages, respectively.

#### A. DIVISION OF THE ORIGINAL IMAGE INTO SUB-IMAGES

AEIHE initially divides the input image into several sub-images to magnify the local information richness and simultaneously preserve the local structure of the input image. This approach aims to address the drawback of global enhancement, that is, executing an enhancement process over the entire image by using its global characteristics while ignoring its local characteristics. However, ignoring these “dominant” local characteristics can distort the image structure and amplify noise (for cases where the image is greatly affected by unwanted noise) in the resultant image. In the first stage, AEIHE assumes that the main ROIs are located at the center of the image, which will be the main focus of the enhancement process, and that the background regions are located at the left and right sides of this image, which are assumed to be less important than the ROIs. Therefore, the details, information richness, and image structure in ROIs can be properly enhanced.

The division procedure depends on the image dimensions (i.e., width (W) and height (H)). The width of the left sub-image is set within 25% of the whole image from its leftmost side, whereas the width of the right sub-image is set within 25% of the whole image from its rightmost side. The remaining width of the image (i.e., 50% at the center of the image) is set as the width of the center sub-image. All sub-images are of the same height as the original image. Therefore, the sizes of the left, center, and right sub-images are  $(H, W/4)$ ,  $(H, W/2)$ , and  $(H, W/4)$ , respectively. For example, assume that the dimension of the input image is (600,900) pixels. In this case, the size of the left and right sub-images is (600,225) pixels, whereas that of the center sub-image is (600,450) pixels. Fig. 8 presents the process of dividing the original image into three sub-images, whereas Figs. 9 (a), (b), and (c) present the coordinates of these sub-images, respectively.

#### B. PARAMETERS INITIALIZATION AND OPTIMIZATION

After the image division stage, all sub-images are individually enhanced and given their specific optimum  $CL_{FACTOR}$  and WS values, which are independent of each other. Obtaining the optimum input values for CLAHE is a subjective issue that requires experience and skill from users.

Therefore, to reduce human intervention and dependency, AEIHE applies the WOA algorithm to automatically and adaptively obtain the optimum values of both  $CL_{FACTOR}$  and WS. The block diagram and pseudocode for applying the WOA algorithm are shown in Figs. 10 and Fig. 11, respectively.

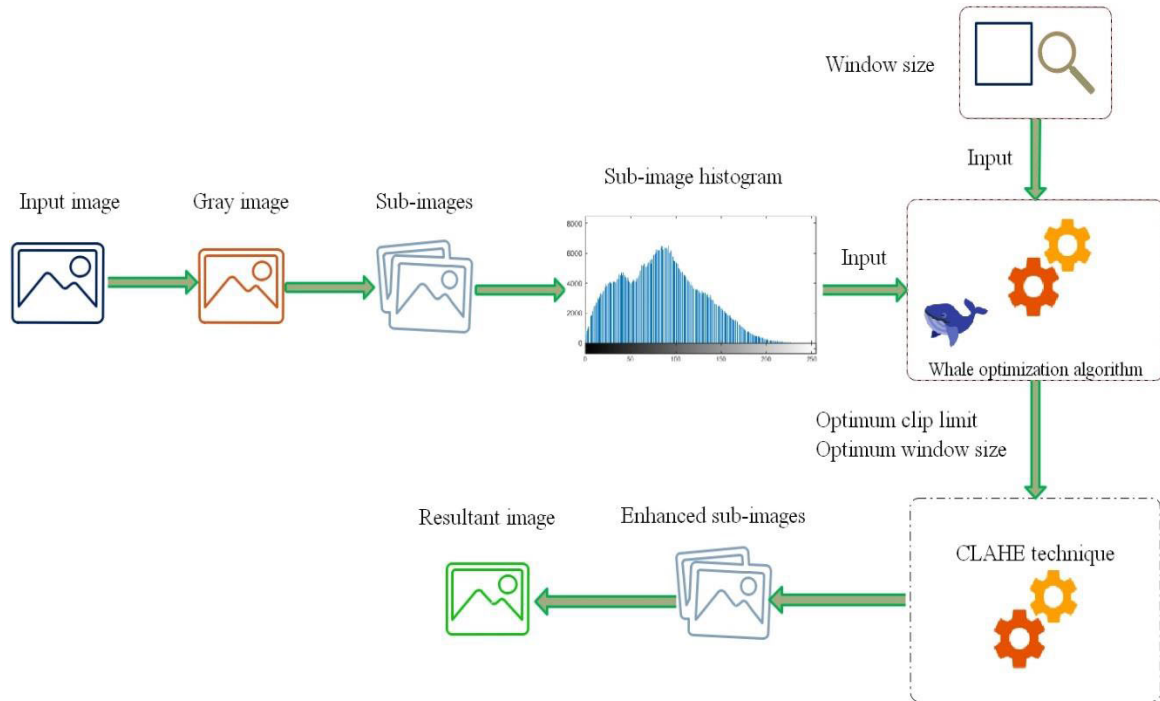


**FIGURE 6.** Process design of the proposed AEIHE technique.

The inputs for the WOA algorithm include the histogram of the sub-image and four predetermined *WS* values (i.e., which are set as initial *WS* values). AEIHE assumes that the contextual regions (i.e., represented by *WS*) can be adaptively set to one of four even values, namely, 4, 6, 8, and 10, and the other even values outside this range are neglected. These four values are chosen based on the following pre-analyzed criteria: the division of the sub-image into two windows (i.e., *WS* = 2) will barely enhance the contrast and the local details, and a higher value (i.e., *WS* = 12 and above) will divide the sub-image into a large number of contextual regions, which can lead to over-enhancement. Based on the histogram of the sub-image and the *WS* values that are used as inputs in the WOA algorithm, six main parameters are identified at this stage, namely, *best\_Entropy-Index*, *best\_CLFACTOR*, *best\_WS*, *CLFACTOR*, *WS*, and *Entropy-Index*. The exploration and exploitation search mechanisms of WOA are used to determine the optimized gray level from the input histogram of a sub-image. Afterward, *CLFACTOR* is computed as

$$CLFACTOR = \frac{H(j)}{\sum_{i=0}^{L-1} H(i)} \quad i, j = 0, 1, 2, 3 \dots L - 1 \quad (1)$$

where  $H(j)$  and  $\sum_{i=0}^{L-1} H(i)$  refer to the number of pixels of the selected (optimized) gray level  $j$  and the total number of pixels of the sub-image histogram, respectively, and *CLFACTOR* is the normalized clip limit whose value is within the range of [0,1]. Consider a simple histogram of one arbitrary sub-image containing several gray-level intensities, namely, 10, 25, 40, 76, 134, 205, and 236, as shown in Fig. 12.

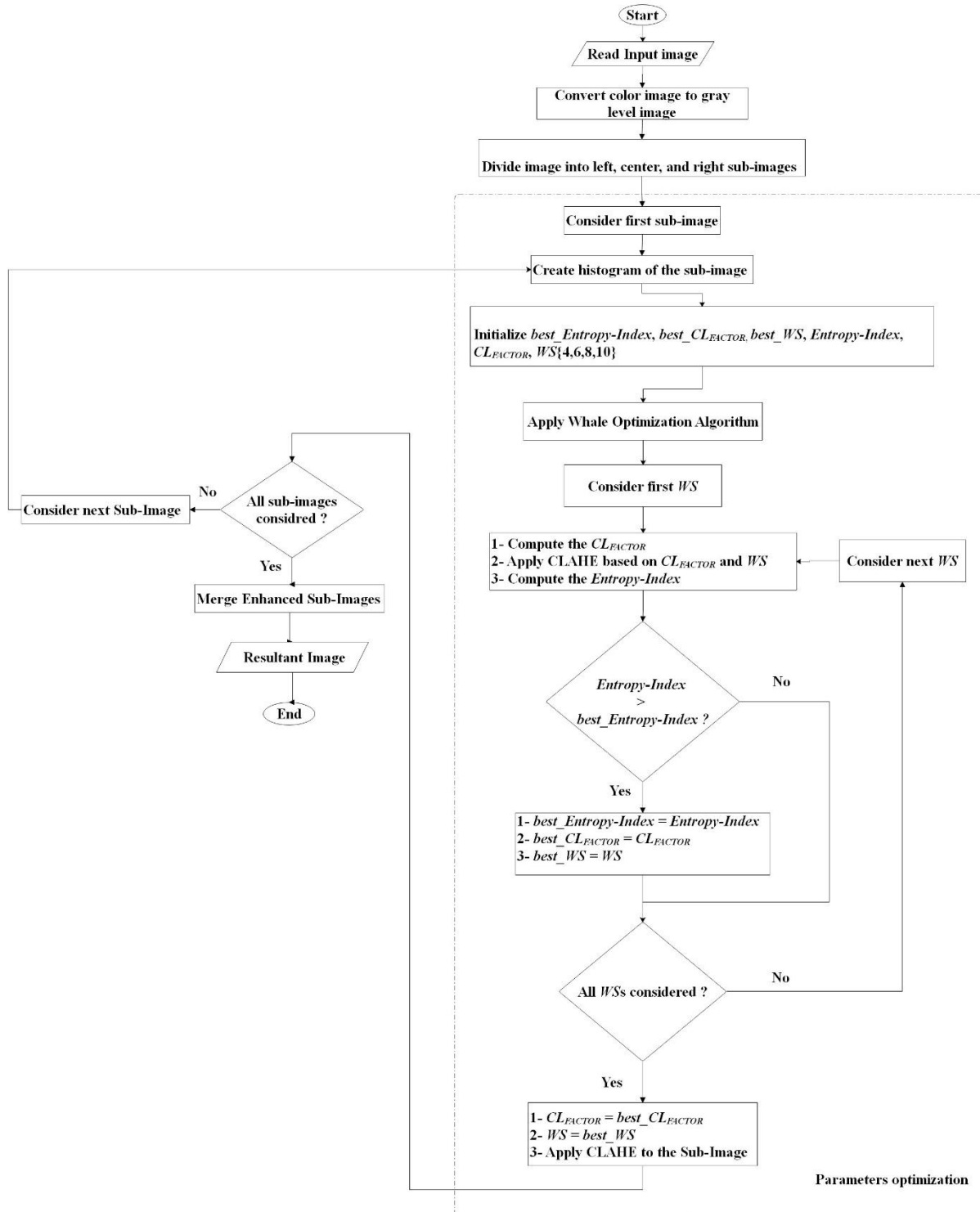
**TABLE 3.** Example of the *CLFACTOR* values of selected gray levels.

The optimized gray levels	Number of pixels for the optimized grey levels, $H(j)$	Total number of pixels in the sub-image, $\sum_{i=0}^{L-1} H(i)$	<i>CLFACTOR</i>
10	100	2000	0.050
40	500	2000	0.250
205	74	2000	0.037

In addition, assume that the number of pixels for these gray levels is 100, 260, 500, 314, 484, 74, and 268, respectively. This histogram will then be applied as an input in the WOA to determine the optimized gray level intensities. Based on the histogram shown in Fig. 12, assume that the optimized gray levels obtained from the WOA algorithm are 10, 40, and 205. Afterward, the *CLFACTOR* is computed by using Equation (1), and the results are tabulated in Table 3. Each *CLFACTOR* value is then combined with all *WS* values (i.e., 4, 6, 8, and 10) and applied to CLAHE to perform the contrast enhancement process. To ensure that the WOA algorithm will produce the optimum *CLFACTOR* value, a new fitness function called *Entropy\_Index* is introduced to this algorithm. This function is computed as

$$Entropy - Index = Entropy \times SSI \quad (2)$$

where *Entropy* and *SSI* refer to the richness of information in the image and the similarity index of the structures of the original and resultant images, respectively.

**FIGURE 7.** Flowchart of the proposed AEIHE technique.

According to Equation (2), the *Entropy-Index* fitness function is specifically devised to enhance and highlight the local details and information richness of a sub-image without distorting its structure. Highlighting and enhancing local

details and information richness are ascertained by the parameter Entropy, whereas preventing the distortion of the sub-image structure is ascertained by the parameter *SSI*. Therefore, the WOA algorithm indirectly requires high

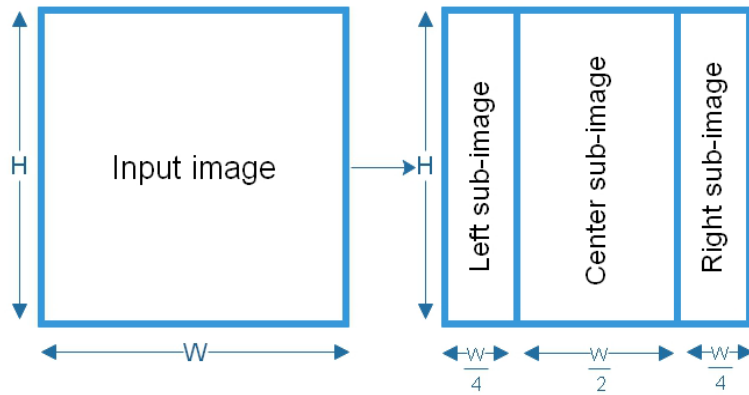


**FIGURE 8.** Division of an input image into three sub-images (i.e., left, center and right sub-images).

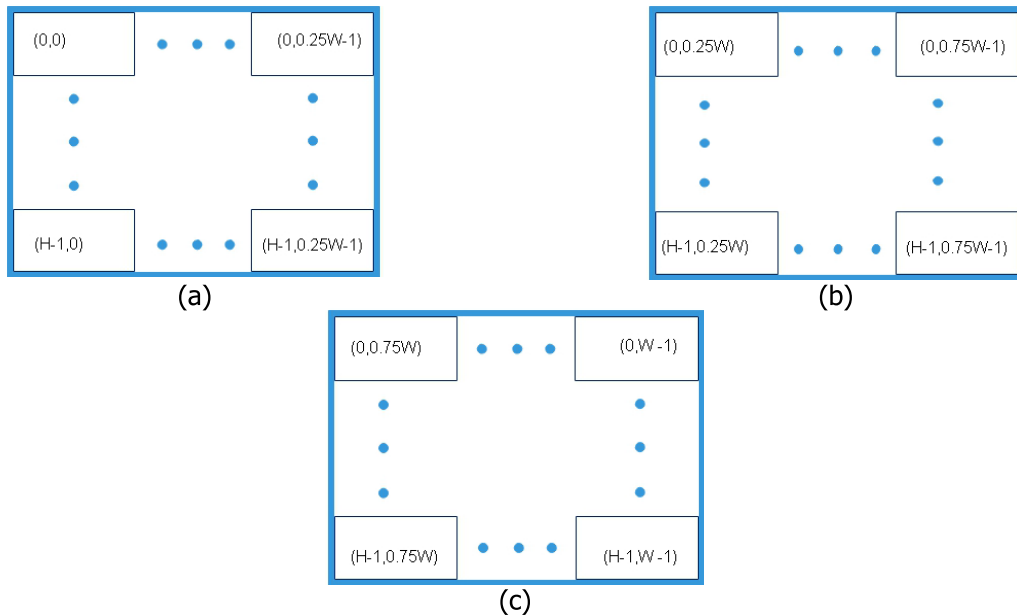


**FIGURE 9.** Pixels coordinates for (a) left sub-image, (b) center sub-image, and (c) right sub-image.

*Entropy* and *SSI* values to obtain the best or highest *Entropy-Index* value. A high *Entropy* value ensures that the local details and information richness are highlighted and enhanced, whereas a high *SSI* value ensures that the sub-image structure is not distorted. Table 4 shows the level (i.e., low, medium, and high) of *Entropy-Index* value that can be derived from four different combinations of *Entropy* and *SSI* levels (i.e., low and high).

To further demonstrate the idea of obtaining the best *Entropy-Index* of all sub-images, the computed  $CL_{FACTOR}$  values for all sub-images are tabulated in Table 5, and each of these values will be combined with four *WS* values. As indicated by the pseudo code of the WOA algorithm in Fig. 11, each *Entropy-Index* value will be compared with the *best\_Entropy-Index* value, and the largest value will be stored as the new *best\_Entropy-Index* value along with its corresponding  $CL_{FACTOR}$  and *WS* as the *best\_CLFACTOR* and

**TABLE 4.** Level of Entropy-Index for different combinations between Entropy and SSI.

Entropy	SSI	Entropy-Index
Low	Low	Low
Low	High	Medium
High	Low	Medium
High	High	High

*best\_WS*, respectively. *Entropy-Index* ensures that improving the information details of the enhanced image will not affect the image structure by preserving the maximum value of *SSI* as the main parameter in the fitness function. Only the combination of high *Entropy* and high *SSI* values will fulfill

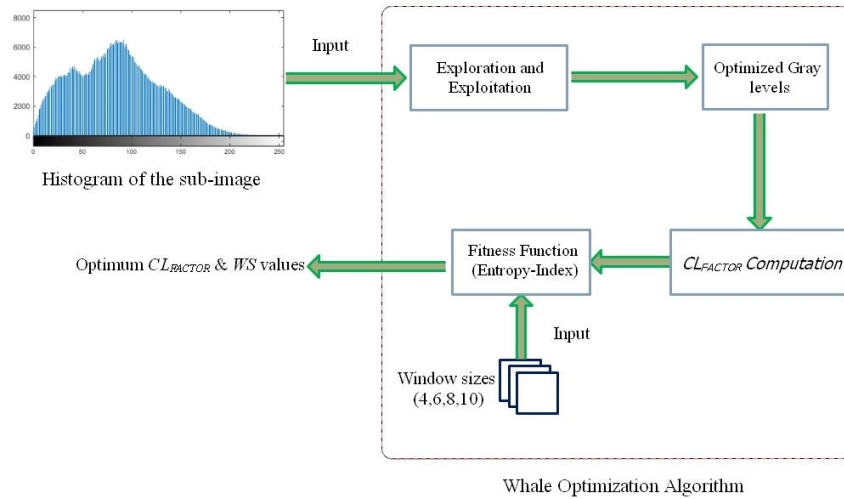


**FIGURE 10.** Block diagram of the WOA algorithm to produce the optimum  $CL_{FACTOR}$  and  $WS$  values.

```

1:   Begin
2:       Compute the Histogram of the Sub-Image
3:       Initialize the lower bound =0, upper bound = 255, Search agents (Populations) of the WOA, Iterations,
   WS( $J$ ) = {4,6,8,10}, best_Entropy-Index =0 , best_CLFACTOR =0, best_WS = 0,  $CL_{FACTOR}$ ,  $WS$ , Entropy-Index
4:   For Iteration  $\leftarrow 1$ 
5:       The search agents move randomly along the histogram of the sub-image according to the moving
   equation of the WOA algorithm
6:       The agents select random gray level
7:       Compute the  $CL_{FACTOR}$  of the selected gray level using Equation (1)
8:       For 4  $\leftarrow J = 1$ 
9:           Apply CLAHE based on the combination of computed  $CL_{FACTOR}$  and  $WS(J)$ 
10:          Compute Entropy-Index using Equation (2)
11:          If Entropy-Index > best_Entropy-Index
12:              best_Entropy-Index = Entropy-Index,
13:              best_CLFACTOR =  $CL_{FACTOR}$ ,
14:              best_WS =  $WS(J)$ 
15:          End if
16:      End For
17:  End For
  
```

**FIGURE 11.** Pseudo code of the WOA algorithm to produce the optimum  $CL_{FACTOR}$  and  $WS$  values.

the maximum fitness function requirements of the WOA algorithm. Table 5 shows that the left sub-image has the *best\_Entropy-Index* value with *WS* and *CLFACTOR* values of 4 and 6.720, respectively, the center sub-image has the *best\_Entropy-Index* value by adopting a *WS* value of 6 and a *CLFACTOR* value of 7.214, and the right sub-image has the *best\_Entropy-Index* value by adopting a *WS* value of 8 and a *CLFACTOR* value of 4.893. The optimum or best values will be

used as input parameters for the conventional CLAHE in the next stage to enhance all sub-images and produce the final resultant image.

#### C. CONSTRUCTION OF THE RESULTANT IMAGE

After obtaining the *best\_CLFACTOR* and *best\_WS* in the second stage, both of these values are used as input parameters to the conventional CLAHE to enhance the contrast of

**TABLE 5.** The relationship between  $WS$ , *Entropy-Index*, and  $CL_{FACTOR}$  for simulation data. (Note: The bolded values represent the best values).

Sub-Image	$CL_{FACTOR}$	Window Size ( $WS$ )	<i>Entropy-Index</i>
Left Sub-Image	0.0035	4	<b>6.720</b>
		6	6.700
		8	6.596
		10	6.597
		4	5.783
	0.036	6	4.967
		8	6.249
		10	5.783
		4	6.891
		6	6.584
Center Sub-Image	0.013	8	7.011
		10	6.517
		4	6.792
		6	<b>7.214</b>
		8	7.001
	0.046	10	6.739
		4	3.673
		6	3.436
		8	3.784
		10	4.104
Right Sub-Image	0.04	4	4.582
		6	4.813
		8	<b>4.893</b>
		10	3.996

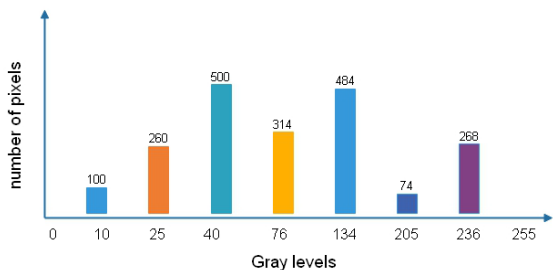


**FIGURE 12.** Example of histogram of an arbitrary sub-image.

each sub-image. Using the *best\_CLFACTOR* and *best\_WS* values associated with the *best\_Entropy-Index* value can produce an enhanced sub-image with an optimum contrast and local detail enhancement, preserved structure, and minimum amplification of unwanted noise. These optimum enhanced sub-images are combined in the dimension process, which is similar to the division process. In other words, the left sub-image is combined with the center sub-image, which in turn is combined with the right sub-image to form the resultant enhanced image. Fig. 13 illustrates the pseudo-code of AEIHE.

#### IV. CONTRIBUTION OF AEIHE TECHNIQUE

Section III has stated that the proposed AEIHE technique is an adaptive version of the conventional CLAHE. The distribution of gray level intensities is not homogenous throughout

```

1: Begin
2: Read input image.
3: Convert color image to gray level image.
4: Divide the image into three sub-images. // left, center and right sub-images
5: For all sub-images do
6: Apply WOA algorithm to find the optimum  $CL_{FACTOR}$  and  $WS$ 
7: Apply the conventional CLAHE technique to produce the optimum enhanced sub-image
8: End do
9: Merge all enhanced sub-images to produce the resultant image
10: End

```

**FIGURE 13.** Pseudo code of the proposed AEIHE technique.

the entire range of an image with non-uniform illumination, which can result in the low contrast of local details in some regions. Therefore, AEIHE divides this image into three sub-images and applies adaptive  $CL_{FACTOR}$  and  $WS$  values for each sub-image until the best contrast enhancement result is achieved. This technique aims to enhance local details and achieve a high level of information richness. AEIHE also ensures the enlargement of low-intensity distribution to the entire gray-level intensity range of a sub-image, the production of the best local details, and the preservation of the image structure.

AEIHE also ensures the production of best-enhanced images without artifacts, unwanted noise, and under- and over-enhancement. This technique uses the new image quality factor (i.e., *Entropy-Index*) to highlight the hidden details and preserve the image structure. AEIHE also ensures the enhancement of the local details in an image and produces an enhanced contrast across its entire area. The clip limit and  $WS$  values for each sub-image are calculated adaptively. The clip boundary of the sub-image is initially calculated in iterative mode, and the optimum value is used to produce the enhanced sub-image. The optimum value of the clip is then combined with the iterative value.

Table 6 shows that AEIHE does not inherit the disadvantages of the conventional CLAHE based on the following justifications:

- i. AEIHE achieves local enhancement by applying an enhancement process on the sub-images. Meanwhile, the conventional CLAHE applies a global enhancement process that can produce over- and under-enhancement problems as reported in previous works [2], [4], and [5].
- ii. AEIHE automatically and adaptively determines the values of parameters. Meanwhile, the conventional CLAHE manually computes these values by trial and error, which is subjective to the skills and knowledge of users and is very time consuming. In some cases, this subjective process may also generate poor values that can lead to a poor enhancement result. AEIHE reduces this subjectivity problem and the amount of time needed to obtain

**TABLE 6.** Comparison between the proposed AEIHE and the CLAHE techniques.

Features	Proposed AEIHE technique	Conventional CLAHE
Determination of $CL_{FACTOR}$ and $WS$	<ul style="list-style-type: none"> <li>Automatically and adaptively determined.</li> <li>More objective and less processing time.</li> <li>Low probability of determining poor value.</li> </ul>	<ul style="list-style-type: none"> <li>Manually determined.</li> <li>Subjective and time-consuming.</li> <li>High probability of determining poor value.</li> </ul>
Introduction of sub-images	<ul style="list-style-type: none"> <li>Input image is divided into sub-images before divided into contextual regions.</li> <li>Provide better enhancement and improvement of the local details.</li> </ul>	<ul style="list-style-type: none"> <li>Not available.</li> <li>Enhancement process is applied globally, thus, enhancement of local details is not properly implemented.</li> </ul>
Introduction of <i>Entropy-Index</i>	<ul style="list-style-type: none"> <li>As fitness function to evaluate the enhancement performance</li> <li>Assist in obtaining the optimum contrast enhancement.</li> <li>Assist in preserving the image's structure.</li> <li>Assist in highlighting the local details of the image.</li> </ul>	<ul style="list-style-type: none"> <li>Not available.</li> </ul>

the optimum values by applying the WOA technique. AIEHE also follows an adaptive process in determining the parameter values for different images.

iii. AEIHE preserves the structure of an image, highlights its local details, and achieves an optimum contrast enhancement by introducing a new fitness function called Entropy-Index, which is not available in the conventional CLAHE.

Based on the abovementioned criteria, AEIHE is expected to produce better resultant images compared with state-of-the-art techniques, especially the conventional CLAHE.

## V. DATASETS AND EVALUATION METRICS

A test is conducted on 1 standard image and 819 sample images to evaluate the performance of AEIHE. The selected images include 1 Lena image, 241 images from the Pasadena-Houses 2000 dataset (size:  $1760 \times 1168$ ) [68], 450 images from the faces 1999 dataset (size:  $896 \times 592$ ) [69], and 89 images from the DIARETDB1 dataset (size:  $1500 \times 1100$ ) [70]. These dataset images are collected from the databases of Image Processing Place, California Institute of Technology, and Standard Diabetic Retinopathy and are chosen based on the large range of information available in these images and their ROI distribution. This study examines the capabilities of AEIHE by conducting a real medical case study focusing on chromosome images. A total of 39 chromosome images (size:  $1376 \times 1024$ ) were collected from Advanced Medical and Digital Images, Universiti Sains Malaysia. For analysis purposes, this study focuses only on

grayscale images, and the tested techniques are applied in the spatial domain and are derived from the conventional HE.

AEIHE is compared with 11 state-of-the-art techniques, namely, DCLHE [12], MVSIHE [19], HSQHE [36], GHE [8], CLAHE [38], BBHE [13], POSHE [39], BPDHE [9], RSWHE [31], the technique proposed in [34], and IAECHE [5], which are selected on the following bases: (i) AEIHE and these techniques work in the spatial domain and are derived from the conventional HE; (ii) the selected techniques follow the same concept as AEIHE, in which the input image is divided into sub-images before its enhancement; (iii) the selected techniques can preserve or enhance the image details; and (iv) MVISHE, [11], DCLHE, and IAECHE are the latest HE-based contrast enhancement techniques that have been published in 2017, 2018, 2019, and 2020, respectively.

Qualitative and quantitative analyses are conducted to evaluate the performance of AEIHE. These analyses focus on (i) contrast-enhancing capabilities, (ii) image brightness, (iii) preservation of information, (iv) image structure, and (v) naturalness of an image. The qualitative evaluation focuses on the visual quality of the resultant images, which are visually inspected for their over-enhancement, contrast improvement, and naturalness. This subjective assessment aims to confirm whether these images have improved contrast and appearance and whether their details and naturalness have been maintained without introducing artifacts [13]. The noise level of the input image should be lowered or at least preserved throughout the enhancement process. Overall, visual assessment is an effective quality measure used for evaluating

the performance of AEIHE [13]. DE, AMBE, PSNR, CII, SSI, and RMSE are quantitative evaluation factors that are used to evaluate AEIHE by using various HE-based derived techniques.

DE is used to calculate the richness of information contained in an image [13]. A high entropy value means that the image contains rich and valuable information. DE can be calculated as follows:

$$DE = - \sum_{l=0}^{L-1} p(l) \cdot \log_2(p(l)) \quad (3)$$

where  $p(l)$  denotes the PDF of the image histogram,  $l$  represents the intensity level in the image histogram, and AMBE represents the capability of AEIHE to maintain the mean image brightness [12]. AMBE can be calculated as the mean difference in brightness between the original and resultant images:

$$M(O) = \frac{1}{NM} \sum_{n=1}^N \sum_{m=1}^M O(n, m) \quad (4)$$

$$M(R) = \frac{1}{NM} \sum_{n=1}^N \sum_{m=1}^M R(n, m) \quad (5)$$

$$AMBE = |M(O) - M(R)| \quad (6)$$

where  $N$  and  $M$  are the rows and columns of the image, respectively, and  $M(O)$  and  $M(R)$  are the mean brightness values of the original and the resultant image.

PSNR, which evaluates the improvement between the resultant and the original images, calculates the degree of degradation based on mean square error (MSE) [14]:

$$MSE = \frac{1}{NM} \sum_{n=1}^N \sum_{m=1}^M [I_i(n, m) - I_o(n, m)]^2 \quad (7)$$

$$PSNR = 10 \log_{10} \left( \frac{(Max(I_i))^2}{MSE} \right) \quad (8)$$

where  $(Max(I_i))^2$ ,  $N$ , and  $M$  refer to the maximum gray-level intensity of the original image  $I_i$ , its rows, and its columns, respectively, and  $I_i(n, m)$  and  $I_o(n, m)$  refer to the intensity values of the original and resultant image pixels, respectively. MSE is used to compute for the mean difference in the intensities of the original and resultant images. Degradation shows a positive relationship with MSE value, that is, a large degradation value indicates a higher degradation in the enhanced image than in the original image. Equations (7) and (8) indicate that PSNR is inversely related to MSE (i.e., PSNR can reach its maximum value with the minimum MSE value) [15].

CII evaluates the percentage of contrast improvement in the enhanced image compared with that in the original image and can be expressed as follows [16]:

$$CII = \frac{C_{enhanced}}{C_{original}} \quad (9)$$

where  $C_{enhanced}$  and  $C_{original}$  denote the average contrast values for the ROIs in the improved and original images,

respectively. The image contrast can be computed as

$$C = \frac{m - a}{m + a} \quad (10)$$

where  $m$  and  $a$  refer to the mean gray levels of the object in the image and the surrounding region, respectively.

SSI indicates the similarity between two images. The value of this parameter should be within the range of [0,1]. An SSI value of 1 indicates that the image structure is not distorted and that the resultant image maintains its original structure. By contrast, a difference is observed between the structures of the original and resultant images when the SSI value is 0. A large SSI value generally indicates a perfect, unmodified image structure [9]. SSI can be computed as

$$\mu_a = \frac{1}{T} \sum_{i=1}^T A_i \quad \mu_b = \frac{1}{T} \sum_{i=1}^T B_i \quad (11)$$

$$\sigma_a^2 = \frac{1}{T-1} \sum_{i=1}^T (A_i - \bar{A})^2 \quad (12)$$

$$SSI(a, b) = \frac{(2\mu_a\mu_b + c1)(2\sigma_{ab} + c2)}{(\mu_a^2 + \mu_b^2 + c1)(\sigma_a^2 + \sigma_b^2 + c2)} \quad (13)$$

where  $\mu_a$  and  $\mu_b$  represent the averages of images  $a$  and  $b$ ,  $\sigma_a^2$  and  $\sigma_b^2$  represent the variances of these images, and  $c1$  and  $c2$  are small constants in the equation.

RMSE denotes the root MSE between the input and enhanced resultant image. RMSE shows an inverse relationship with the quality of the resultant image. In other words, a low RMSE value indicates that the resultant image has a higher quality and lower distortion in its details and information compared with the input image [8], [33]. RMSE can be computed as

$$RMSE = \sqrt{\frac{\sum_{i=1}^N \sum_{j=1}^M (A(i, j) - B(i, j))^2}{N \times M}} \quad (14)$$

where  $i$  and  $j$  refer to the image rows and columns, and  $N$ ,  $M$ ,  $A(i, j)$ , and  $B(i, j)$  denote the rows and columns of the input and resultant images.

The proposed AEIHE technique and all the compared techniques were implemented on Intel i5 2.5 GHz, RAM 16G, SSD hard disk and by using MATLAB R2019a.

## VI. RESULTS AND DISCUSSION

Qualitative and quantitative analyses are performed to demonstrate the capability of AEIHE. This technique is compared with 11 state-of-the-art techniques, namely, DCLHE [12], MVIHE [19], HSQHE [36], GHE [8], CLAHE [38], BBHE [13], POSHE [39], BPDHE [9], RSWHE [31], the technique proposed in [34], and IAECHE [5], all of which have been implemented by using their optimum parameters as suggested by their respective authors. The results of the qualitative analysis are presented and discussed by using one standard image and one image from each dataset (i.e., Pasadena-Houses 2000, faces 1999, DIARETDB1, and chromosomes datasets) as presented in

**TABLE 7.** Quantitative evaluation of Lena image. (Note: The bold and underline fonts refer to the best and second-best values, respectively.)

Technique	DE	PSNR	SSI	AMBE	CII	RMSE
DCLHE	7.238	22.439	<b>0.989</b>	<u>7.877</u>	1.017	9.578
MVSIHE	7.032	<b>32.509</b>	<u>0.981</u>	<b>3.753</b>	<u>1.050</u>	5.781
HSQHE	7.497	28.857	0.874	8.543	1.018	5.414
GHE	5.936	14.971	0.802	31.772	<b>1.059</b>	13.272
CLAHE	7.810	17.504	0.727	19.746	1.033	12.170
BBHE	7.129	16.651	0.758	16.686	1.015	10.808
POSHE	7.814	19.430	0.760	14.830	1.029	7.238
BPDHE	7.108	19.123	0.860	13.949	0.922	9.369
RSWHE	6.372	24.528	0.743	7.261	0.865	<u>4.602</u>
[34]	7.448	20.446	0.915	20.689	0.999	7.518
IAECHE	<u>7.563</u>	22.218	0.930	11.872	1.012	10.583
Proposed AEIHE	<b>7.669</b>	<u>27.694</u>	0.945	9.685	0.972	<b>4.031</b>

Figs. 14, 16, 19, 22, and 24, respectively. The images from these datasets are labelled Lena, Pasadena01, Faces01, DIARETDB101 and Chromosomes01. Fig. 15 presents the magnified region of the Lena image, Figs. 17 and 18 show two magnified areas of Pasadena01, Figs. 20 and 21 present the magnified areas of Faces01, and Fig. 23 displays the magnified area of DIARETDB101. The quantitative results for these five images as tabulated in Tables 7 to 11 are used to support the qualitative assessment. The bold and underlined numbers in these tables indicate the best and second-best results, respectively. Table 12 presents the average results for the quantitative analyses of all tested datasets, and Table 13 presents the results of the computational time analysis.

The results of the qualitative analysis for the Lena image as obtained by AEIHE and the other techniques are shown in Fig. 14. For further analysis, the magnified area of the resultant Lena image as indicated by the blue box is shown in Fig. 15. DCLHE and MVSIHE barely enhance the image, especially the details of the woman's hat and hair, as shown in Figs. 14(b) and (c), respectively. These techniques are also unable to address the darkness in the image as shown in the face and wall regions behind the woman. The magnified blue region clearly shows that the resultant images of both DCLHE and MVSIHE suffer from blur effects, which can lead to the dimming or deletion of local details as shown in Figs. 15(b) and (c), respectively. The resultant image of HSQHE suffers from unwanted artifacts and texture distortion, especially on the shoulder and face of the woman. In other words, HSQHE is unable to enhance and improve the local image details as shown in Fig. 14(d). Furthermore, the texture of the hat in the magnified blue area is not properly highlighted and has a poor visual appearance as shown in Fig. 15(d). The resultant images of GHE and BBHE in Figs. 14(e) and 14(g), respectively, are affected by unpleasant appearance and over-brightness problems. In addition, the magnified areas of these images as shown in Figs. 15(e) and 15(g) prove that GHE and BBHE are

also affected by the brightness problem, which leads to the vanishment of the hat's details.

The resultant image obtained by CLAHE suffers from an over-enhancement problem as shown in Fig. 14(f), whereas those obtained by POSHE and BPDHE, as shown in Figs. 14(h) and (i), respectively, are affected by unwanted artifacts as can be observed in the area above the hat and on the woman's face and shoulder. The details of the woman's hair are also distorted. The magnified areas of these images reveal that some image details have gone missing, thereby highlighting the limitation of these techniques in improving and enhancing the local details of images.

The resultant Lena image obtained by RSWHE shows distorted details and unwanted artifacts on the right side and on the shoulder of the woman as shown in Fig. 14(j). The resultant magnified image is affected by the darkening and vanishment of details problems as shown in Fig. 15(j), both of which result in the unnatural appearance of the image. By contrast, the resultant image produced by the technique proposed in [33] as shown in Fig. 14(k) faces an over-brightness or over-enhancement problem as can be clearly observed in the shoulder area and from the unnatural appearance of the woman's hair. AEICHE is slightly able to preserve the brightness of the image and improve its local details as shown in Fig. 14(l). The magnified region in this image shows that AEICHE is slightly capable of improving the local details of the hat. Figs. 14(m) and 15(m) prove that AEIHE can produce better resultant images. AEIHE also successfully preserves the image brightness and highlights its local details, especially the lip, hair, and face regions of Lena and the texture of the hat. The resultant images are very natural and pleasant to the human eye. The capability of AEIHE in improving and preserving the richness of information in the image is reflected in its second highest DE value as tabulated in Table 7. Although CLAHE obtains the highest DE, the qualitative analysis shows that this technique suffers from the over-enhancement problem, which corrupts the image details. This problem is successfully addressed by



**FIGURE 14.** Resultant image of Lena after applying with (a) Original image, (b) DCLHE, (c) MVIHE, (d) HSQHE, (e) GHE, (f) CLAHE, (g) BBHE, (h) POSHE, (i) BPDHE, (j) RWSHE, (k) technique from [34], (l) IAECHE, (m) Proposed AEIHE.

AEIHE. In addition, AEIHE obtains the lowest RMSE and the third highest PSNR, thereby proving that this technique is not sensitive to noise effects.

The qualitative analysis results for the Pasadena01 image are shown in Fig. 16. Two magnified regions, as represented by the blue and red boxes in Figs. 17 and 18, are considered for further qualitative analysis. The resultant image obtained by DCLHE, MVIHE, and HSQHE as shown in Figs. 16(b), (c), and (d) reveal that these techniques barely enhance the image, specifically its local details, such as the grass in front of the house, the lines of the brick wall, the leaves of the trees, and the pavement in front of the main entrance to the house. DCLHE, MVIHE, and HSQHE have also failed to improve

the image brightness, and certain local and small details have been dimmed. Furthermore, the resultant images obtained by these techniques show distortions on the upper left and right sides of the sky. The blue magnified region shows that the details of the window curtain, window frame, and brick borders as shown in Figs. 17(b), (c), and (d) have not been preserved by these techniques. From the magnified region of the resultant image as denoted by red, one can see that the left side of the house is blurred and that the details of the tree, including its leaves and branches, can barely be discerned as shown in Figs. 18(b), (c), and (d), respectively. Four other state-of-the-art techniques, namely, GHE, CLAHE, BBHE, and POSHE, produce unnatural and unpleasant resultant

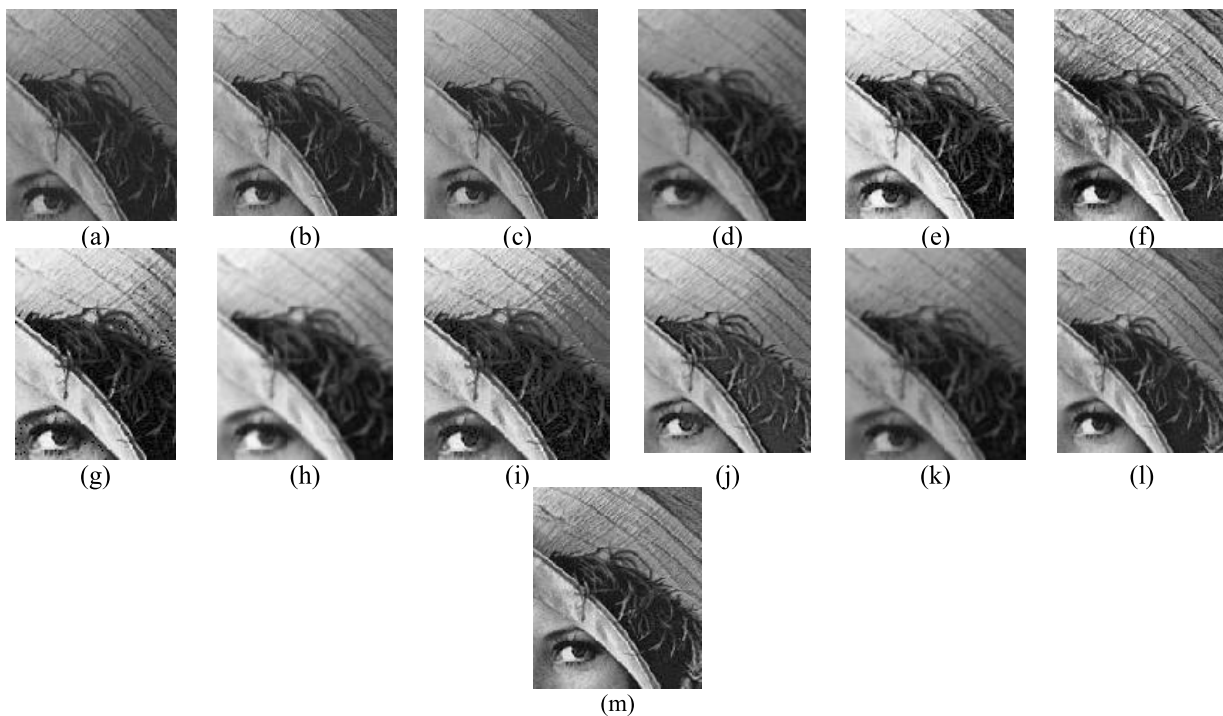


**FIGURE 15.** Magnified red boxed area of Lena after applying with (a) Original image, (b) DCLHE, (c) MVIHE, (d) HSQHE, (e) GHE, (f) CLAHE, (g) BBHE, (h) POSHE, (i) BPDHE, (j) RWSHE, (k) technique from [34], (l) IAECHE, (m) Proposed AEIHE.

images, especially POSHE. The resultant images obtained by these techniques suffer from unwanted artifacts and distortions as clearly observed in the sky region as shown in Figs. 16(e) to (h). The magnified areas of these images as denoted by blue (Figs. 17(e) to (h)) and red (Figs. 18(e) to (h)) further justify the poor enhancement performance of these techniques. The resultant images obtained by BPDHE and RSWHE show slight enhancements as can be seen from the main entrance of the house and the details of its left side. However, the trees behind the house are not clear and have not been properly highlighted, thereby proving that these techniques are not suitable for improving local image details as shown in Figs. 16(i) and (j). Moreover, the bricks surrounding the window and the curtain in the blue magnified area shown in Figs. 17(i) and (j) have been improperly enhanced, and the details of the house wall and trees in the red magnified area shown in Figs. 18(i) and (j) have not been effectively restored.

The resultant image obtained by the technique proposed in [34] is blurred, which leads to the dimness of local details, such as the grass in front of the house, the left side of the house, and the pavement of the main entrance, as shown in Figs. 16(k), 17(k), and 18(k). The resultant image in Fig. 16(l) highlights the ability of IAECHE to improve the image better than the other techniques. This finding can also be justified by the blue and red magnified regions shown in Figs. 17(l) and 18(l), respectively. However, small regions, such as the pavement at the main entrance and the trees on the right side of the image, suffer from over-enhancement.

Specifically, some details of the pavement have vanished, and the leaves of the trees are over-brightened. The resultant image obtained by AEIHE has a natural appearance and brightness. This technique also demonstrates its ability to enhance and highlight local details, such as the grass in front of the house and the pavement at the main entrance. Fig. 16(m) shows that the resultant image has limited to no blur or over-brightness problems, thereby validating the ability of AEIHE to facilitate a consistent and balanced redistribution of image pixels. In addition, the blue magnified area in the resultant image shows that AEIHE can enhance and highlight local details, such as those of the curtain, the window frame, and the lines between the bricks, all of which have been successfully outlined with clear edges. The enhancement of these small regions is not affected by any unwanted noise or artifacts as shown in Fig. 17(m). The red magnified area in the resultant image obtained by AEIHE also shows better improvements without the effects of artifacts as compared with those obtained by the other techniques. For instance, Fig. 18(m) shows that the fence rods and trees in the resultant image obtained by AEIHE are visually clearer and more visible to the human eye compared with those obtained by the other techniques.

The qualitative analysis results for AEIHE are strongly supported by the findings of the quantitative analysis as shown in Table 8. AEIHE obtains the second-best DE value and the best SSI value, thereby indicating that this technique can highlight the information details in an image and maintain its structure much better than the other techniques.

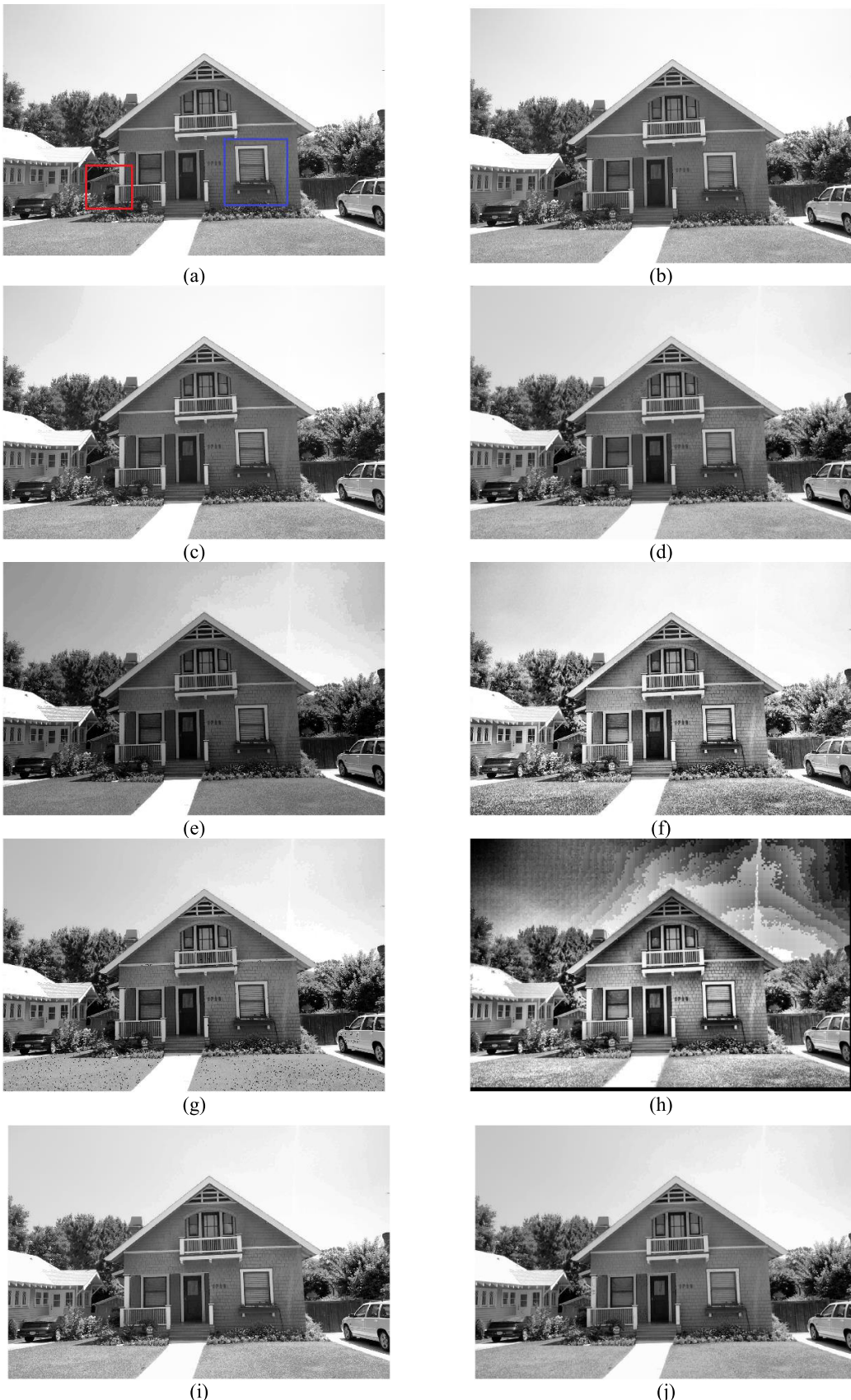


**FIGURE 16.** Resultant image of Pasadena01 after applying with (a) Original image, (b) DCLHE, (c) MVIHE, (d) HSQHE, (e) GHE, (f) CLAHE, (g) BBHE, (h) POSHE, (i) BPDHE, (j) RWSHE, (k) technique from [34], (l) IAECHE, (m) Proposed AEIHE.

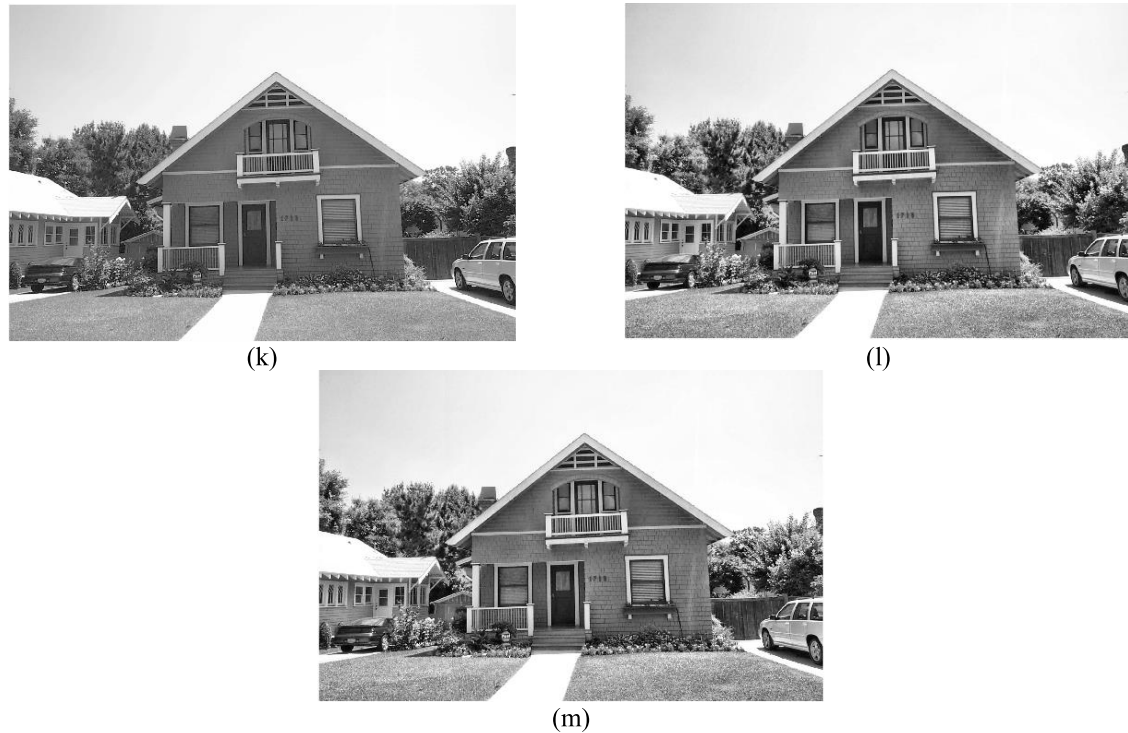


**FIGURE 16.** (Continued.) Resultant image of Pasadena01 after applying with (a) Original image, (b) DCLHE, (c) MVSIEHE, (d) HSQHE, (e) GHE, (f) CLAHE, (g) BBHE, (h) POSHE, (i) BPDHE, (j) RWSHE, (k) technique from [34], (l) IAECHE, (m) Proposed AEIHE.

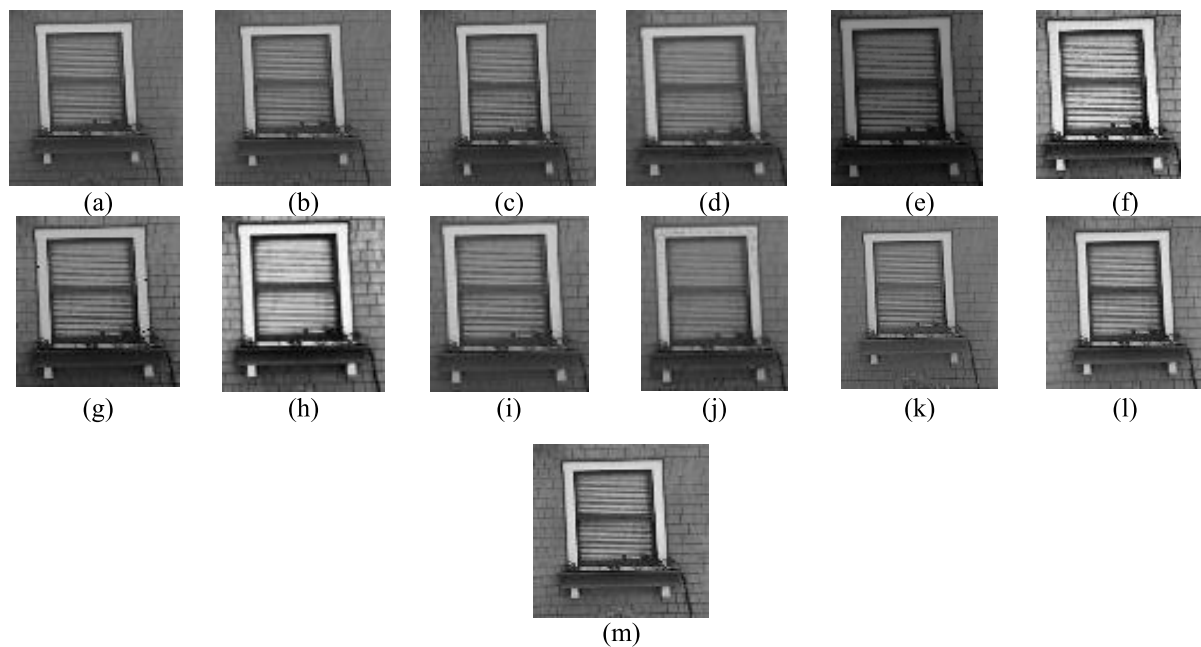


**FIGURE 17.** Magnified blue boxed area of Pasadena01 after applying with (a) Original image, (b) DCLHE, (c) MVSIEHE, (d) HSQHE, (e) GHE, (f) CLAHE, (g) BBHE, (h) POSHE, (i) BPDHE, (j) RWSHE, (k) technique from [34], (l) IAECHE, (m) Proposed AEIHE.

In addition, by having the best PSNR value, AEIHE can reduce the effect of unwanted noise. The results of the qualitative and quantitative analyses also justify that AEIHE produces the best Pasadena01 image among all techniques.

Faces01 is a close-up image taken in an indoor environment. This image has poorly illuminated regions with hidden local details. Similar to Pasadena01, the resultant images obtained by DCLHE, MVSIEHE, and HSQHE have

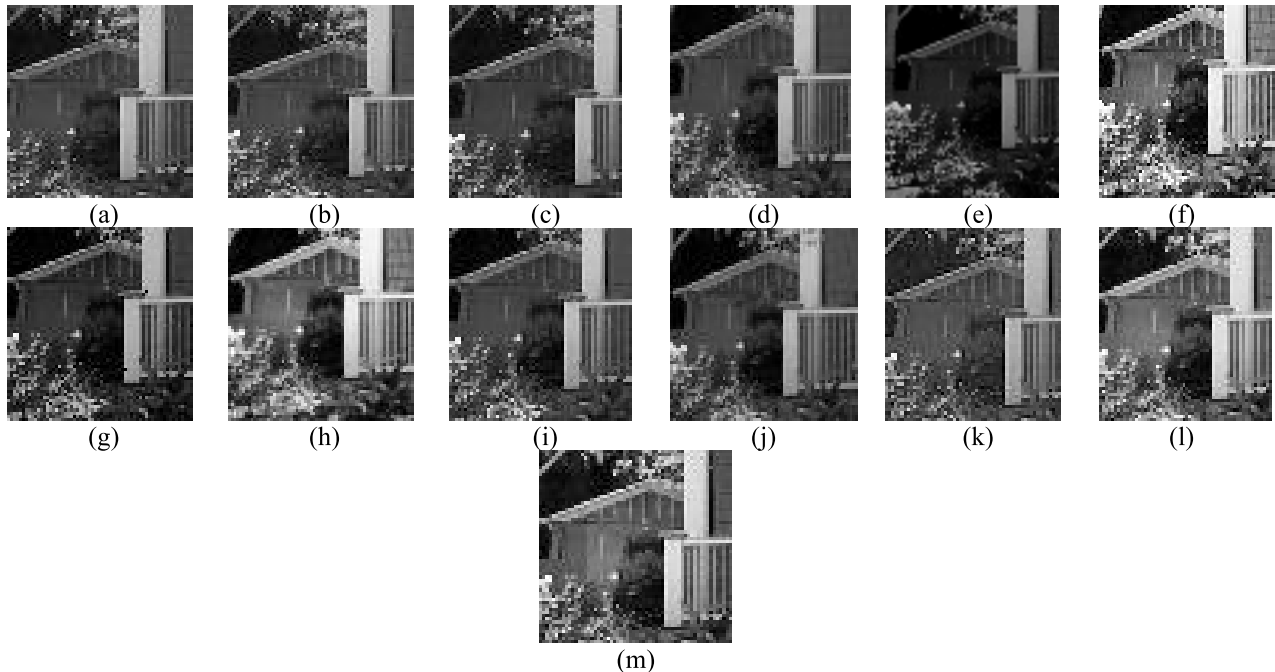


**FIGURE 18.** Magnified red boxed area of Pasadena01 after applying with (a) Original image, (b) DCLHE, (c) MVSIE, (d) HSQHE, (e) GHE, (f) CLAHE, (g) BBHE, (h) POSHE, (i) BPDHE, (j) RWSHE, (k) technique from [34], (l) IAECHE, (m) Proposed AEIHE.

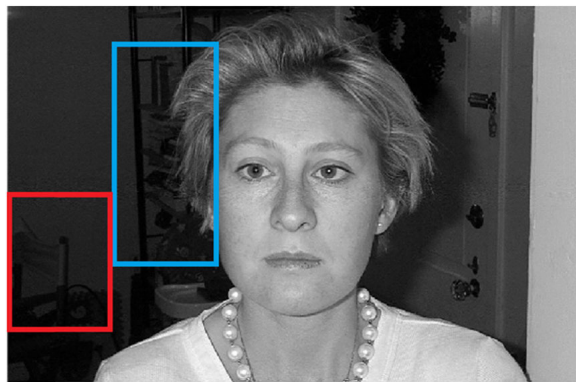
**TABLE 8.** Quantitative evaluation of Pasadena01 image. (Note: The bold and underline fonts refer to the best and second-best values, respectively.)

Technique	DE	PSNR	SSI	AMBE	CII	RMSE
DCLHE	6.972	29.920	<u>0.993</u>	1.34	1.000	<b>1.450</b>
MVSIE	6.591	27.323	0.989	1.965	1.000	<u>2.428</u>
HSQHE	7.374	27.014	0.938	5.544	1.030	3.922
GHE	5.728	15.691	0.874	38.481	0.962	8.352
CLAHE	7.565	19.195	0.863	6.019	1.031	9.072
BBHE	6.972	21.559	0.878	13.828	<b>1.048</b>	2.657
POSHE	<b>9.251</b>	7.845	0.701	43.157	0.936	8.365
BPDHE	7.015	29.908	0.677	1.981	1.018	3.317
RWSHE	7.374	27.014	0.544	1.938	<u>1.034</u>	2.734
[34]	7.142	<u>30.693</u>	0.821	<b>1.16</b>	0.974	9.072
IAEACHE	7.463	23.967	0.954	6.885	1.000	2.917
Proposed AEIHE	<u>7.929</u>	<b>32.109</b>	<b>0.999</b>	4.452	1.000	3.240

barely been improved. Specifically, these techniques have not improved the brightness of the image, which has led to a dim resultant image as shown in Figs. 19(b) to (d), respectively. In addition, white spots are observed on the surface area of the resultant image obtained by MVSIE. These techniques also fail to highlight local and hidden details in the magnified areas (Figs. 20(b), (c), and (d) and Figs. 21(b), (c), and (d)). These regions suffer from poor illumination and brightness improvements, and the bottles on the shelves cannot be discerned as shown in Figs. 20(b), (c), and (d). Similar results can be observed from the red magnified region of this image due to poor contrast as shown in Figs. 21(b), (c), and (d). The resultant images obtained by GHE, POSHE, and BPDHE suffer from over-brightness, hence explaining the missing details

on the woman's face as shown in Figs. 19(e), (h), and (i). The blue (Figs. 20(e), (h), and (i)) and red magnified areas (Figs. 21(e), (h), and (i)) of these images also show that the texture and details of the woman's hair and the naturalness of the chair on the left side have not been retained by these techniques.

Figs. 19 to 21 show that the resultant images obtained by CLAHE, BBHE, and the technique proposed in [34] suffer from over-enhancement, hence making these images unpleasant to the human eye (see (f), (g), and (k) of these figures). This problem can also be clearly observed from the red magnified areas, which show an improper brightness (Figs. 21(f), (g), and (k)). Among the 11 state-of-the-art techniques being compared, only RWSHE, IAEACHE, and



(a)



(b)



(c)



(d)



(e)



(f)



(g)



(h)

**FIGURE 19.** Resultant image of Faces01 after applying with (a) Original image, (b) DCLHE, (c) MVIHE, (d) HSQHE, (e) GHE, (f) CLAHE, (g) BBHE, (h) POSHE, (i) BPDHE, (j) RWSHE, (k) technique from [34], (l) IAECHE, (m) Proposed AEIHE.



**FIGURE 19.** (Continued.) Resultant image of Faces01 after applying with (a) Original image, (b) DCLHE, (c) MVIHE, (d) HSQHE, (e) GHE, (f) CLAHE, (g) BBHE, (h) POSHE, (i) BPDHE, (j) RWSHE, (k) technique from [34], (l) IAECHE, (m) Proposed AEIHE.

AEIHE obtain resultant images without (or nearly without) poorly illuminated or over-enhanced areas, especially on the woman's face, as shown in Figs. 19(j), (l), and (m), respectively. These techniques also successfully highlight local details on the image as shown in the blue and red magnified areas. The image details and contrast are also enhanced, and the brightness is improved without amplifying noise and adding unwanted artifacts as shown in Figs. 20(j), (l), and (m) for the blue magnified area and Figs. 21(j), (l), and (m) for the red magnified area. AEIHE obtains the best SSI and RMSE values for the Faces01 image as presented in Table 9. These results support the findings of the qualitative analysis that favor AEIHE as the

best technique. These SSI and RMSE values also show that AEIHE is highly capable of enhancing image contrast, producing an excellent resultant image, preserving the image structure, and reducing the effect of unwanted noise. AEIHE also obtains the second-best DE value among the compared techniques and a remarkable PSNR value, hence highlighting its ability to produce signal values without amplifying noise during the enhancement process.

The resultant images and the blue magnified region of the resultant DIARETDB101 images obtained by the compared techniques are shown in Figs. 22 and 23, respectively. The resultant images obtained by DCLHE and the proposed technique in [34] do not show any improvements,

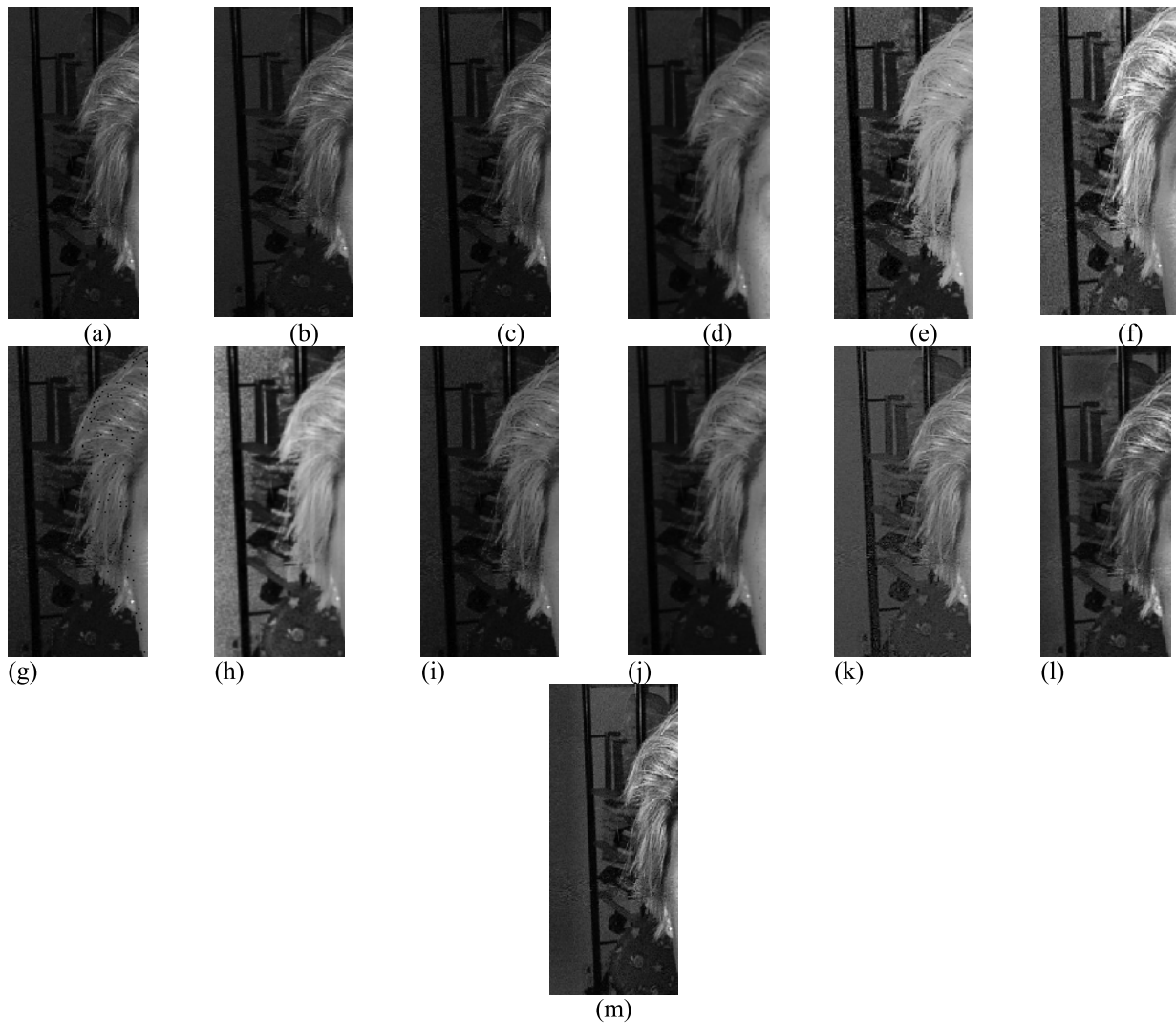


**FIGURE 20.** Magnified blue boxed area of Faces01 after applying with (a) Original image, (b) DCLHE, (c) MVSIE, (d) HSQHE, (e) GHE, (f) CLAHE, (g) BBHE, (h) POSHE, (i) BPDHE, (j) RWSHE, (k) technique from [34], (l) IAECHE, (m) Proposed AEIHE.

**TABLE 9.** Quantitative evaluation of Faces01 image. (Note: The bold and underline fonts refer to the best and second-best values, respectively.)

Technique	DE	PSNR	SSI	AMBE	CII	RMSE
DCLHE	7.489	<b>43.333</b>	<u>0.994</u>	<u>3.672</u>	1.002	3.737
MVSIE	7.308	<u>36.705</u>	0.980	3.145	1.007	3.448
HSQHE	7.619	31.030	0.900	<b>2.750</b>	1.002	5.822
GHE	5.976	15.183	0.763	39.691	1.012	14.977
CLAHE	7.825	16.220	0.657	21.367	<b>1.051</b>	12.702
BBHE	7.226	24.471	0.883	7.402	0.975	8.994
POSHE	<b>10.495</b>	7.805	0.589	37.555	<u>1.045</u>	14.067
BPDHE	7.253	27.095	0.789	6.925	1.008	6.049
RWSHE	7.620	30.420	0.237	4.893	1.032	5.295
[34]	7.651	18.137	0.907	13.820	1.000	3.820
IAEACHE	8.255	25.109	0.82	30.865	1.010	<u>3.201</u>
Proposed AEIHE	<u>8.556</u>	29.647	<b>0.995</b>	6.582	1.010	<b>2.581</b>

and some local details have not been highlighted as shown in Figs. 22(b) and (k). This case is particularly observed in the magnified area shown in Figs. 23(b) and (k), where

the details and contrast of the veins and other local details are not improved. Meanwhile, the resultant images obtained by MVSIE, HSQHE, GHE, CLAHE, BBHE, POSHE,

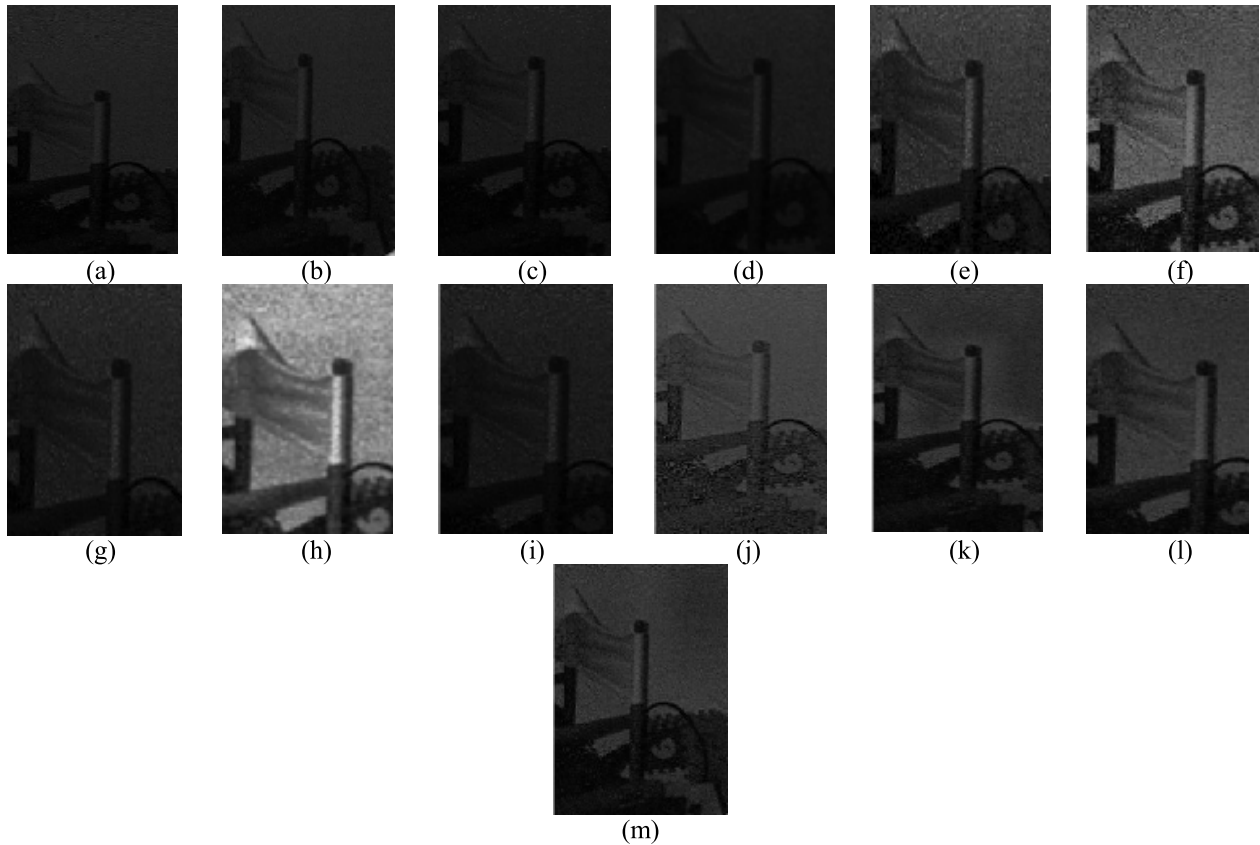


**FIGURE 21.** Magnified red boxed area of Faces01 after applying with (a) Original image, (b) DCLHE, (c) MVSIE, (d) HSQHE, (e) GHE, (f) CLAHE, (g) BBHE, (h) POSHE, (i) BPDHE, (j) RWSHE, (k) technique from [34], (l) IAECHE, (m) Proposed AEIHE.

**TABLE 10.** Quantitative evaluation of DIARETDB101 image. (Note: The bold and underline fonts refer to the best and second-best values, respectively.)

Technique	DE	PSNR	SSI	AMBE	CII	RMSE
DCLHE	6.615	26.100	<u>0.928</u>	11.544	1.009	11.974
MVSIE	6.413	<b>30.684</b>	0.876	6.647	1.019	7.447
HSQHE	7.106	30.501	0.834	2.672	0.952	5.994
GHE	5.665	13.066	0.688	<b>44.838</b>	<u>1.055</u>	14.515
CLAHE	6.867	22.322	0.727	11.857	1.019	11.721
BBHE	6.467	14.486	0.623	27.176	1.019	12.725
POSHE	15.146	7.677	0.542	23.456	1.044	13.004
BPDHE	6.470	13.454	0.722	7.764	<b>1.074</b>	14.156
RWSHE	7.179	26.660	0.815	8.626	1.037	8.636
[34]	<u>7.350</u>	18.796	0.707	7.749	1.046	<u>4.912</u>
IAECHE	6.669	21.265	0.909	6.645	1.000	5.934
Proposed AEIHE	<b>7.651</b>	<u>27.462</u>	<b>0.946</b>	3.980	0.967	<b>4.291</b>

BPDHE, and RWSHE suffer from over-enhancement that leads to over-brightness as shown in Figs. 23(c) to (j), respectively. Among these techniques, POSHE produces the worst resultant image with unsMOOTH texture and obvious over-enhancement problems as shown in Fig. 22(h). Meanwhile, BBHE and RWSHE obtain the second and third worst resultant images as shown in Figs. 22(g) and (j), respectively. The over-enhancement problem faced by these eight techniques can be clearly observed from the magnified area of the

resultant DIARETDB101 image as shown in Figs. 23(c) to (j). A washout problem (which leads to an improper enhancement of image details) can also be observed from this magnified area.

The resultant images obtained by IAECHE and AEIHE are much clearer than those obtained by the other techniques as shown in Figs. 22(l) and (m) and Figs. 23(l) and (m), respectively. The local details have been enhanced without facing an over-enhancement problem or the effects of unwanted noise

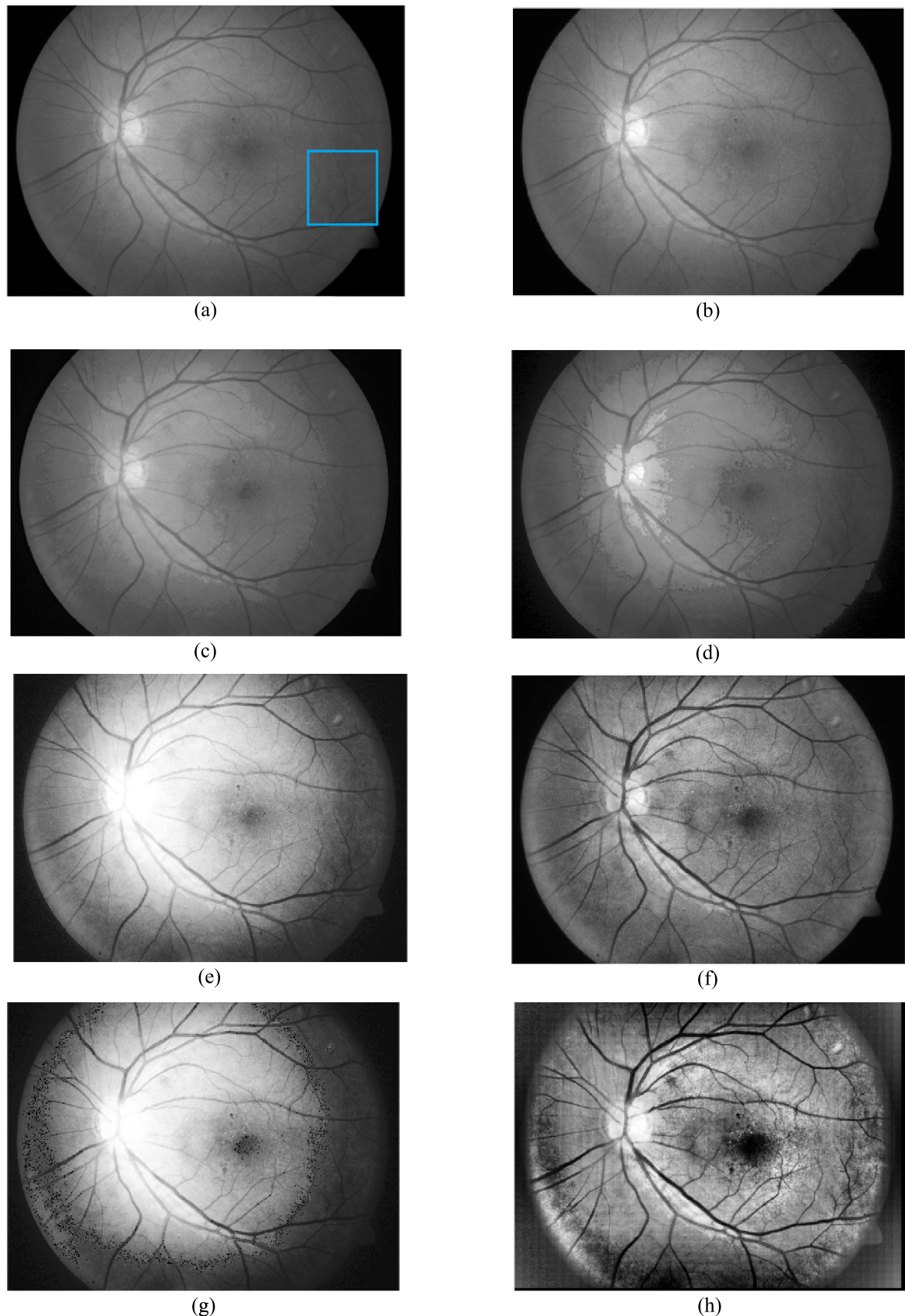


**FIGURE 22.** Resultant image of DIARETDB101 after applying with (a) Original image, (b) DCLHE, (c) MVSIE, (d) HSQHE, (e) GHE, (f) CLAHE, (g) BBHE, (h) POSHE, (i) BPDHE, (j) RWSHE, (k) technique from [34], (l) IAECHE, (m) Proposed AEIHE.

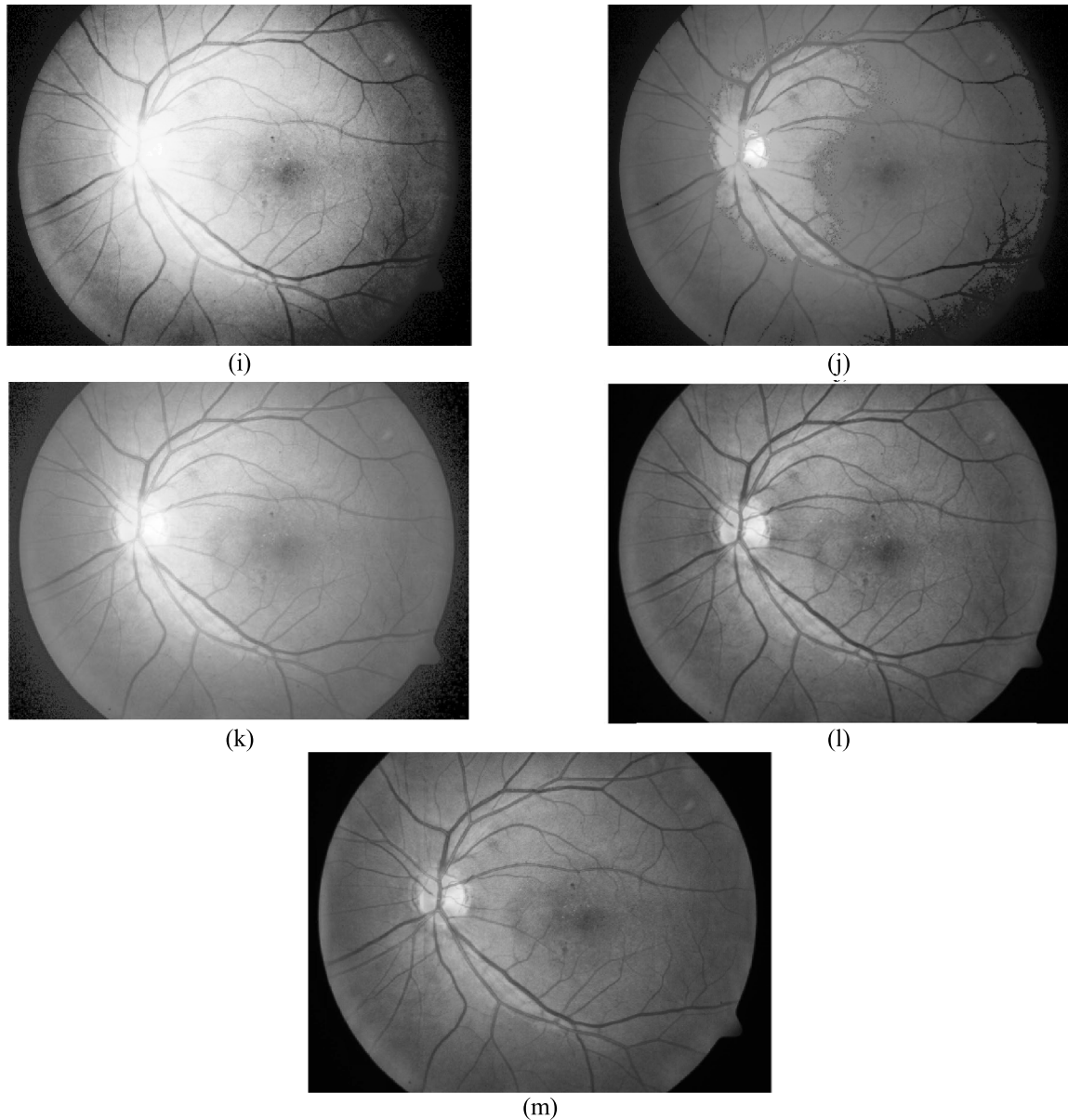


**FIGURE 22. (Continued.)** Resultant image of DIARETDB101 after applying with (a) Original image, (b) DCLHE, (c) MVIHE, (d) HSQHE, (e) GHE, (f) CLAHE, (g) BBHE, (h) POSHE, (i) BPDHE, (j) RWSHE, (k) technique from [34], (l) IAECHE, (m) Proposed AEIHE.

or artifacts. These techniques also demonstrate their ability to control the natural brightness of the image. The eye's texture and veins can be clearly observed. The quantitative analysis results in Table 10 indicate that AEIHE outperforms IAECHE in terms of SSI and RMSE. However, AEIHE only obtains the second-best DE and PSNR values. These findings indicate that AEIHE successfully enhances the information richness and details of the resultant image (i.e., the best DE value), preserves its structure (i.e., the best SSI value), and is less sensitive to the effects of noise (i.e., the best RMSE value and second-best PSNR value).

The resultant Chromosomes01 images obtained by the compared techniques are shown in Fig. 24. A visual

observation of those images obtained by DCLHE, CLAHE, the proposed technique in [34], and IAECHE reveal only a slight enhancement as shown in Figs. 24(b), (f), (k), and (l), respectively. The bonding patterns of the chromosomes are not properly enhanced; thus, the structural details of the chromosomes cannot be observed. Meanwhile, the resultant images obtained by HSQHE, BPDHE, and RSWHE show changes in their background region color (from bright to dark) as can be seen in Figs. 24(d), (i), and (j), respectively. The resultant images obtained by GHE and POSHE suffer from the darkening of chromosome bonds, thereby resulting in poor image quality and unrecognizable chromosome details as shown in Figs. 24(e) and (h), respectively.

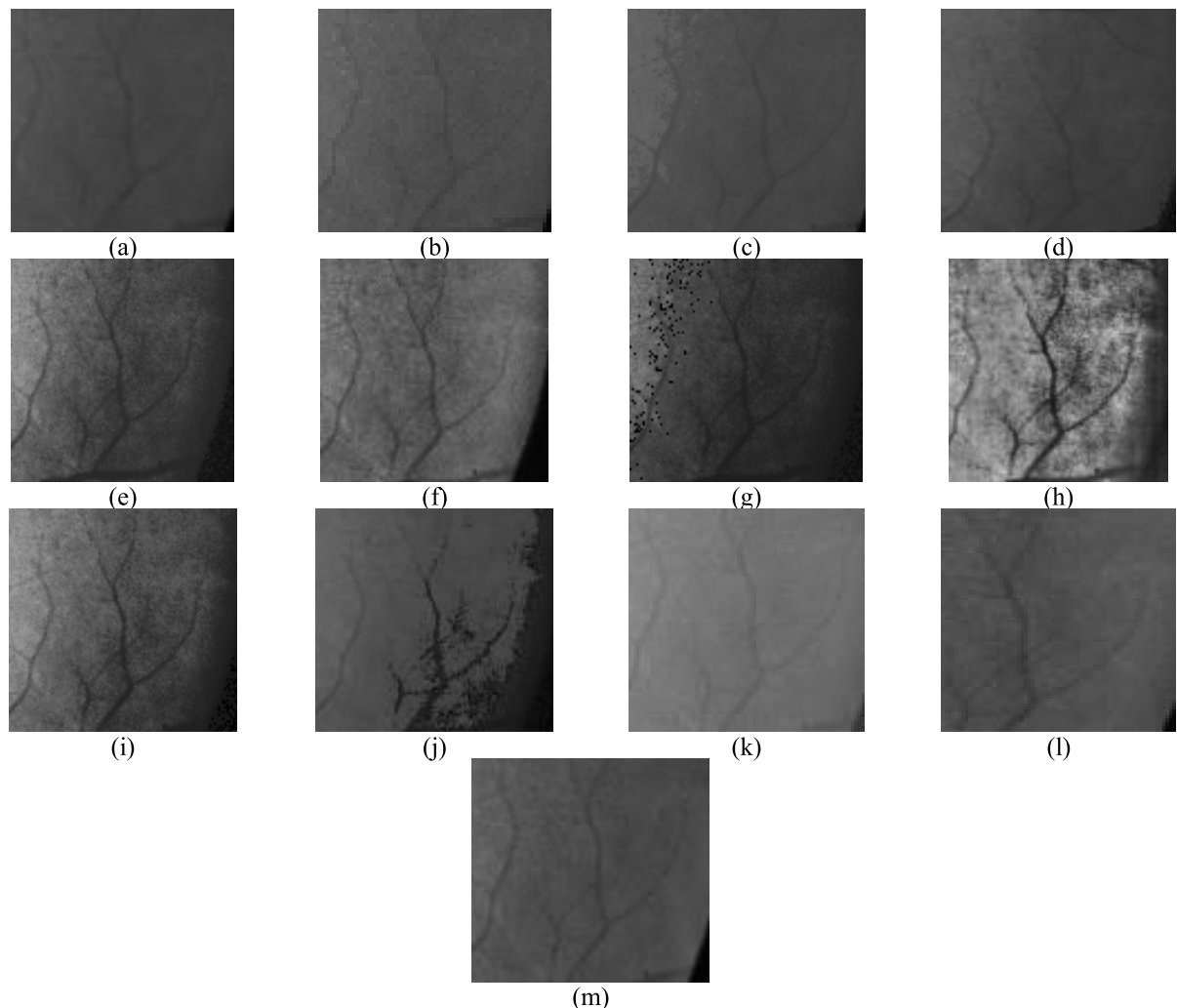


**FIGURE 23.** Magnified blue boxed area of DIARETDB101 after applying with (a) Original image, (b) DCLHE, (c) MVSIE, (d) HSQHE, (e) GHE, (f) CLAHE, (g) BBHE, (h) POSHE, (i) BPDHE, (j) RWSHE, (k) technique from [34], (l) IAECHE, (m) Proposed AEIHE.

**TABLE 11.** Quantitative evaluation of Chromosomes01 image. (Note: The bold and underline fonts refer to the best and second-best values, respectively.)

Technique	DE	PSNR	SSI	AMBE	CHI	RMSE
DCLHE	1.136	24.733	<b>0.999</b>	<u>1.154</u>	1.000	2.072
MVSIE	<u>1.581</u>	<b>58.869</b>	0.963	6.256	0.850	<b>1.042</b>
HSQHE	1.112	14.955	0.936	2.033	0.542	2.190
GHE	0.909	13.245	0.798	3.886	<u>1.047</u>	2.142
CLAHE	1.471	35.843	<u>0.977</u>	2.100	<u>1.089</u>	1.048
BBHE	1.300	23.823	0.927	4.109	<b>1.062</b>	<u>1.047</u>
POSHE	1.563	2.707	0.714	8.392	1.023	1.378
BPDHE	1.113	7.166	0.760	9.235	0.273	1.462
RWSHE	1.478	13.170	0.912	5.104	0.452	2.031
[34]	0.605	<u>45.565</u>	0.067	2.263	0.702	1.053
IAEACHE	1.083	36.55	0.907	<b>1.039</b>	1.000	1.153
Proposed AEIHE	<b>1.613</b>	33.409	<b>0.999</b>	1.333	0.804	1.210

Among the compared state-of-the-art techniques, MVSIE and AEIHE obtain the resultant images with the best contrast. The contrast of the resultant image obtained by AEIHE is slightly lower than that of the image obtained

by MVSIE. However, AEIHE effectively preserves and highlights the bonding and chromosome structures as supported by the results of the quantitative analysis in Table 11, which reveal that AEIHE obtains the best SSI and

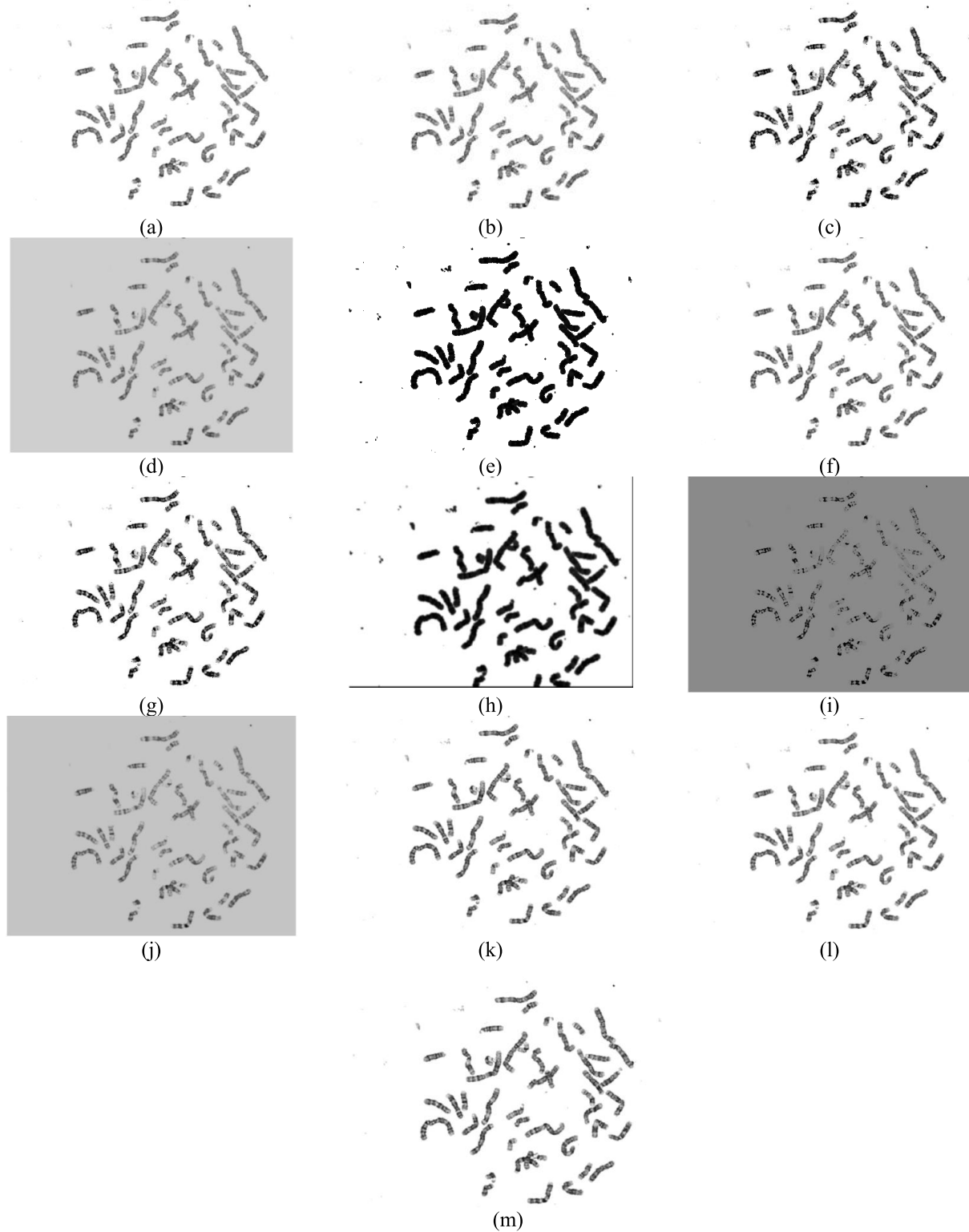


**FIGURE 24.** Resultant image of Chromosomes01 after applying with (a) Original image, (b) DCLHE, (c) MVSIE, (d) HSQHE, (e) GHE, (f) CLAHE, (g) BBHE, (h) POSHE, (i) BPDHE, (j) RWSHE, (k) technique from [34], (l) IAECHE, (m) Proposed AEIHE.

DE values among all techniques. This technique can therefore preserve the structure of the chromosome image, which is important for enhancing contrast and retaining the bonding patterns of the chromosome structure for medical diagnosis purposes.

In addition to the sample images, the average quantitative assessment of the proposed AEIHE technique for all the 819 images is calculated and compared to the other techniques. As mentioned, 241 images from the Pasadena-Houses 2000 dataset (size:  $1760 \times 1168$ ) [68], 450 images from

**TABLE 12.** Average quantitatively evaluation. (Note: The bold and underline fonts refer to the best and second-best values, respectively.)

Datasets	Technique	DE	PSNR	SSI	AMBE	CII	RMSE
Pasadena-Houses 2000	DCLHE	7.465	31.331	<b>0.998</b>	<u>1.468</u>	0.999	<b>2.450</b>
	MVSIHE	7.330	<b>38.259</b>	<u>0.991</u>	<b>1.259</b>	<u>1.013</u>	3.042
	HSQHE	7.574	27.170	0.898	3.372	<b>1.027</b>	8.205
	GHE	5.820	21.491	0.642	7.890	1.012	6.281
	CLAHE	7.285	12.635	0.716	6.605	1.014	9.072
	BBHE	7.236	23.89	0.898	5.898	1.000	<u>2.657</u>
	POSHE	7.468	12.443	0.692	14.30	0.998	8.326
	BPDHE	7.239	25.986	0.943	6.756	1.010	3.317
	RSWHE	<u>7.768</u>	29.786	0.918	3.431	0.998	4.734
	[34]	7.471	25.132	0.931	12.742	1.004	3.621
	IAECHE	7.345	27.000	0.900	7.000	0.980	5.715
	Proposed	<b>7.778</b>	<u>32.534</u>	0.877	6.358	0.990	3.910
faces 1999	AEIHE						
	DCLHE	7.482	<b>42.853</b>	<b>0.997</b>	2.106	1.000	4.420
	MVSIHE	7.297	25.871	<u>0.984</u>	<u>1.609</u>	1.000	5.961
	HSQHE	7.624	29.789	0.897	<b>1.481</b>	1.002	4.210
	GHE	5.943	18.457	0.817	21.211	<b>1.047</b>	6.225
	CLAHE	7.928	12.476	0.473	21.696	<u>1.042</u>	4.234
	BBHE	7.282	21.273	0.834	7.997	1.028	4.319
	POSHE	7.874	14.176	0.720	20.948	1.037	<u>5.624</u>
	BPDHE	6.273	26.844	0.927	6.060	1.0	5.934
	RSWHE	<u>7.861</u>	29.046	0.906	4.592	1.015	6.152
	[34]	7.610	24.274	0.929	15.947	1.000	6.843
	IAECHE	<b>8.000</b>	<u>29.361</u>	9.901	9.125	0.898	<b>3.961</b>
DIARETDB1	Proposed	<u>7.935</u>	24.734	0.903	6.207	0.982	4.853
	AEIHE						
	DCLHE	5.938	18.655	0.802	3.193	<b>1.084</b>	8.013
	MVSIHE	6.484	31.6	0.983	4.9627	0.983	8.282
	HSQHE	6.272	26.635	0.859	<u>2.602</u>	1.008	8.624
	GHE	8.886	5.417	0.473	8.269	1.115	9.421
	CLAHE	6.397	19.812	0.723	5.939	<u>1.045</u>	9.620
	BBHE	5.796	11.126	0.522	5.838	1.043	11.655
	POSHE	<b>7.874</b>	14.176	0.720	2.948	1.037	12.156
	BPDHE	6.273	26.844	0.927	6.060	1.000	14.204
	RSWHE	5.868	<u>29.101</u>	0.917	<b>2.546</b>	0.956	12.207
	[34]	6.540	16.865	0.546	8.110	1.019	15.090
Chromosomes	IAECHE	6.023	22.651	<b>0.932</b>	7.284	1.010	<u>8.013</u>
	Proposed	<u>6.930</u>	<b>29.147</b>	<u>0.885</u>	6.970	0.989	<b>6.341</b>
	AEIHE						
	DCLHE	1.502	<b>49.634</b>	<b>0.999</b>	1.016	0.370	1.011
	MVSIHE	1.439	25.826	0.951	1.037	0.079	<u>0.981</u>
	HSQHE	1.075	16.176	0.654	0.962	<b>0.690</b>	1.184
	GHE	2.318	1.643	0.622	3.572	0.174	1.374
	CLAHE	<b>3.263</b>	30.194	0.970	1.199	0.270	1.381
	BBHE	1.851	25.136	3.872	0.927	0.214	1.399
	POSHE	<u>2.679</u>	5.182	0.374	4.274	0.084	1.467
	BPDHE	1.474	2.784	0.392	4.529	0.535	1.537
	RSWHE	1.083	14.624	0.950	5.054	<u>0.606</u>	1.682
	[34]	0.774	<u>37.532</u>	0.73	<b>0.751</b>	0.026	1.428
AEIHE	IAECHE	1.000	30.239	0.864	<u>0.900</u>	0.239	1.234
	Proposed	1.016	33.158	<u>0.987</u>	1.692	0.591	<b>0.611</b>

the faces 1999 dataset (size:  $896 \times 592$ ) [69], 89 images from the DIARETDB1 dataset (size:  $1500 \times 1100$ ) [70], and 39 images from the chromosome dataset (size:  $1376 \times 1024$ ) are used, and the results are presented in Table 12. AEIHE has been proven to be highly capable of enhancing the information richness and details of images as reflected in

its best DE values for the Pasadena-Houses 2000 dataset and the second-best average DE values for the faces 1999 dataset. AEIHE has also been proven to be less sensitive to the effects of noise and obtains the best average RMSE and PSNR values for the DIARETDB1 dataset, the best average RMSE value for the chromosome dataset, and the second best

**TABLE 13.** Average time consuming.

Dataset	Technique	Average time consuming (Seconds)
Pasadena-Houses 2000	DCLHE	3.2
	MVSIHE	2.4
	HSQHE	4.6
	GHE	1.3
	CLAHE	2.7
	BBHE	1.9
	POSHE	3.2
	BPDHE	2.6
	RSWHE	3.1
	[34]	2.0
	IAECHE	33.6
	Proposed AEIHE	82.1
	DCLHE	2.8
	MVSIHE	2.0
faces 1999	HSQHE	3.8
	GHE	0.9
	CLAHE	3.2
	BBHE	2.6
	POSHE	6.2
	BPDHE	4.7
	RSWHE	3.0
	[34]	2.6
	IAECHE	26.7
	Proposed AEIHE	64.3
	DCLHE	4.2
	MVSIHE	3.8
	HSQHE	3.1
	GHE	1.5
DIARETDB1	CLAHE	2.0
	BBHE	3.2
	POSHE	4.0
	BPDHE	2.7
	RSWHE	2.5
	[34]	3.8
	IAECHE	27.0
	Proposed AEIHE	52.6
	DCLHE	1.8
	MVSIHE	1.4
	HSQHE	1.9
	GHE	0.8
	CLAHE	1.0
	BBHE	1.2
Chromosomes	POSHE	1.7
	BPDHE	1.3
	RSWHE	1.0
	[34]	1.0
	IAECHE	13.3
	Proposed AEIHE	19.3

average PSNR value for the Pasadena-Houses 2000 dataset. The introduction of Entropy-Index improves the capability of AEIHE in preserving image details as reflected in its second-best average SSI value for the DIARETDB1 and chromosome datasets. The results of the qualitative and quantitatively analyses favor AEIHE as an excellent HE-based technique for enhancing image contrast. AEIHE has successfully

produced resultant images with favorable contrast improvements, information richness and details, and excellently preserved structure with minimal effects from noise, unwanted artifacts, and over-enhancement.

This study further analyzes and evaluates the performance of AEIHE via a computational time analysis, and the results are shown in Table 13. GHE, BBHE, DCLHE, and MVSIHE

are capable of completing the enhancement process within a short period. By contrast, AEIHE requires the longest computational time due to its implementation of iteration processes in obtaining the optimum parameter values. However, despite this limitation, the visual and quantitative analyses have proven that AEIHE is highly capable of producing excellent and natural resultant images with high image quality values. Therefore, with further improvements, especially a reduced computational time, AEIHE shows great potential to be used for enhancing image contrast in non-real-time applications.

## VII. LIMITATIONS AND FUTURE WORK

In the present days image processing applications can be classified into real-time and non-real-time applications, with the former requiring the application of image processing techniques that are computationally fast and have short execution times, such as video streaming, outland drones patrol, and military applications. By contrast, non-real time applications, such as medical imaging and using personal cameras, do not highly depend on time when processing images but rather focus on the production of optimum results. Although the available approaches for real-time applications can rapidly produce outputs, in some cases, these approaches demonstrate poor performance and are unable to produce the optimum results, whereas the approaches for non-real time applications may consume a high processing time yet can produce the optimum results in some cases. The proposed AEIHE is specifically designed for non-real-time applications and focuses on obtaining optimum resultant images that are natural and pleasant to the human eye with enhanced local details, preserved structure, and low sensitivity to noise effects.

After its capabilities has been proven in this study, future work should focus on improving and modifying AEIHE in order for this technique to be used in real-time applications. To do so, future studies may adaptively identify the optimum WS value in order for AEIHE to automatically test each pre-determined WS value (which can consume much time when done manually). Another possible direction for improving AEIHE is introducing an adaptive procedure to divide the input image into multiple sub-images. Three possible ideas can be implemented. First, AEIHE should be able to adaptively identify the optimum number of sub-images to be created. Second, the improved AEIHE should also be able to adaptively identify the size of each sub-image. Third, the improved AEIHE technique should be applied to the RGB images and enhance the color images.

## VIII. CONCLUSION

This paper proposes an adaptive version of the conventional CLAHE technique to enhance image contrast in the spatial domain. The proposed technique, called AEIHE, is specifically designed to produce images with high contrast, clear local details, and preserved structure. A new assessment parameter called Entropy-Index is also introduced to obtain the best entropy and structural similarity values.

This parameter is used as a fitness function for the WOA algorithm to obtain the best clip limit value for the conventional CLAHE. AEIHE is tested on 819 images from 4 datasets, and its performance is compared with that of 11 state-of-the-art techniques. The qualitative and quantitative analysis results prove that AEIHE outperforms the other techniques and may produce natural images. The high DE value obtained by AEIHE demonstrate its capability of enhancing images and producing a high level of information, particularly local image details. AEIHE can also maintain the natural brightness of images and produce a high information signal without any unwanted noise and artifacts. Overall, AEIHE is capable of enhancing the contrast, detail, and structure of images, thereby highlighting its potential to be applied in the machine vision, medical imaging, and industrial fields.

## REFERENCES

- [1] S. Sridhar, *Digital Image Processing*, 2nd ed. New Delhi India: Oxford Univ. Press, 2011.
- [2] H. Lidong, Z. Wei, W. Jun, and S. Zebin, "Combination of contrast limited adaptive histogram equalisation and discrete wavelet transform for image enhancement," *IET Image Process.*, vol. 9, no. 10, pp. 908–915, Oct. 2015, doi: [10.1049/iet-ipr.2015.0150](https://doi.org/10.1049/iet-ipr.2015.0150).
- [3] R. C. Gonzalez, R. E. Woods, and S. L. Eddins, *Digital Image Processing*, vol. 2, 2nd ed. Upper Saddle River, NJ, USA: Prentice-Hall, 2002.
- [4] M. Agarwal and R. Mahajan, "Medical image contrast enhancement using range limited weighted histogram equalization," *Procedia Comput. Sci.*, vol. 125, pp. 149–156, 2018, doi: [10.1016/j.procs.2017.12.021](https://doi.org/10.1016/j.procs.2017.12.021).
- [5] S. H. Majeed and N. A. M. Isa, "Iterated adaptive entropy-clip limit histogram equalization for poor contrast images," *IEEE Access*, vol. 8, pp. 144218–144245, 2020.
- [6] W. Z. W. Ismail and K. S. Sim, "Contrast enhancement dynamic histogram equalization for medical image processing application," *Int. J. Imag. Syst. Technol.*, vol. 21, no. 3, pp. 280–289, Sep. 2011, doi: [10.1002/ima.20295](https://doi.org/10.1002/ima.20295).
- [7] M. Tuba, M. Jordanski, and A. Arsic, *Improved Weighted Thresholded Histogram Equalization Algorithm for Digital Image Contrast Enhancement Using the Bat Algorithm*. Amsterdam, The Netherlands: Elsevier, 2016.
- [8] R. C. Gonzalez and R. E. Woods, *Digital Image Processing Using MATLAB*, 2nd ed. New Delhi India: Pearson, 2004.
- [9] H. Ibrahim and N. Pik Kong, "Brightness preserving dynamic histogram equalization for image contrast enhancement," *IEEE Trans. Consum. Electron.*, vol. 53, no. 4, pp. 1752–1758, Nov. 2007, doi: [10.1109/TCE.2007.4429280](https://doi.org/10.1109/TCE.2007.4429280).
- [10] X. Wang and L. Chen, "Contrast enhancement using feature-preserving bi-histogram equalization," *Signal, Image Video Process.*, vol. 12, no. 4, pp. 685–692, 2017, doi: [10.1007/s11760-017-1208-2](https://doi.org/10.1007/s11760-017-1208-2).
- [11] M. Abdullah-Al-Wadud, "A modified histogram equalization for contrast enhancement preserving the small parts in images," *Int. J. Comput. Sci. Netw. Secur.*, vol. 12, no. 2, pp. 1–4, 2012.
- [12] E. Reddy and R. Reddy, "Dynamic clipped histogram equalization technique for enhancing low contrast images," *Proc. Nat. Acad. Sci., India A, Phys. Sci.*, vol. 89, no. 4, pp. 673–698, Dec. 2019, doi: [10.1007/s40010-018-0530-6](https://doi.org/10.1007/s40010-018-0530-6).
- [13] Y.-T. Kim, "Contrast enhancement using brightness preserving bi-histogram equalization," *IEEE Trans. Consum. Electron.*, vol. 43, no. 1, pp. 1–8, 1997, doi: [10.1109/30.580378](https://doi.org/10.1109/30.580378).
- [14] Y. Wang, Q. Chen, and B. Zhang, "Image enhancement based on equal area dualistic sub-image histogram equalization method," *IEEE Trans. Consum. Electron.*, vol. 45, no. 1, pp. 68–75, Feb. 1999, doi: [10.1109/30.754419](https://doi.org/10.1109/30.754419).
- [15] S.-D. Chen and A. R. Ramli, "Minimum mean brightness error bi-histogram equalization in contrast enhancement," *IEEE Trans. Consum. Electron.*, vol. 49, no. 4, pp. 1310–1319, Nov. 2003, doi: [10.1109/TCE.2003.1261234](https://doi.org/10.1109/TCE.2003.1261234).
- [16] K. G. Dhal and S. Das, "Combination of histogram segmentation and modification to preserve the original brightness of the images," *Pattern Recognit. Image Anal.*, vol. 27, no. 2, pp. 200–212, Apr. 2017, doi: [10.1134/S1054661817020031](https://doi.org/10.1134/S1054661817020031).

- [17] S. H. Lim, N. A. Mat Isa, C. H. Ooi, and K. K. V. Toh, "A new histogram equalization method for digital image enhancement and brightness preservation," *Signal, Image Video Process.*, vol. 9, no. 3, pp. 675–689, Mar. 2015.
- [18] C. Zuo, Q. Chen, and X. Sui, "Range limited bi-histogram equalization for image contrast enhancement," *Optik*, vol. 124, no. 5, pp. 425–431, Mar. 2013, doi: [10.1016/j.ijleo.2011.12.057](https://doi.org/10.1016/j.ijleo.2011.12.057).
- [19] L. Zhuang and Y. Guan, "Image enhancement via subimage histogram equalization based on mean and variance," *Comput. Intell. Neurosci.*, vol. 2017, pp. 1–12, 2017, doi: [10.1155/2017/6029892](https://doi.org/10.1155/2017/6029892).
- [20] K. G. Dhal, A. Das, S. Ray, J. Gálvez, and S. Das, "Histogram equalization variants as optimization problems: A review," *Arch. Comput. Methods Eng.*, to be published, doi: [10.1007/s11831-020-09425-1](https://doi.org/10.1007/s11831-020-09425-1).
- [21] P. Babu and V. Rajamani, "Contrast enhancement using real coded genetic algorithm based modified histogram equalization for gray scale images," *Int. J. Imag. Syst. Technol.*, vol. 25, no. 1, pp. 24–32, Mar. 2015, doi: [10.1002/ima.22117](https://doi.org/10.1002/ima.22117).
- [22] S.-D. Chen and A. R. Ramli, "Contrast enhancement using recursive mean-separate histogram equalization for scalable brightness preservation," *IEEE Trans. Consum. Electron.*, vol. 49, no. 4, pp. 1301–1309, Nov. 2003, doi: [10.1109/TCE.2003.1261233](https://doi.org/10.1109/TCE.2003.1261233).
- [23] K. S. Sim, C. P. Tso, and Y. Y. Tan, "Recursive sub-image histogram equalization applied to gray scale images," *Pattern Recognit. Lett.*, vol. 28, no. 10, pp. 1209–1221, Jul. 2007, doi: [10.1016/j.patrec.2007.02.003](https://doi.org/10.1016/j.patrec.2007.02.003).
- [24] K. Singh and R. Kapoor, "Image enhancement via median-mean based sub-image-clipped histogram equalization," *Optik*, vol. 125, no. 17, pp. 4646–4651, Sep. 2014, doi: [10.1016/j.ijleo.2014.04.093](https://doi.org/10.1016/j.ijleo.2014.04.093).
- [25] P. Kandhway and A. K. Bhandari, "An optimal adaptive thresholding based sub-histogram equalization for brightness preserving image contrast enhancement," *Multidimensional Syst. Signal Process.*, vol. 30, no. 4, pp. 1859–1894, Oct. 2019, doi: [10.1007/s11045-019-00633-y](https://doi.org/10.1007/s11045-019-00633-y).
- [26] M. Abdullah-Al-Wadud, M. Kabir, M. Akber Dewan, and O. Chae, "A dynamic histogram equalization for image contrast enhancement," *IEEE Trans. Consum. Electron.*, vol. 53, no. 2, pp. 593–600, May 2007, doi: [10.1109/TCE.2007.381734](https://doi.org/10.1109/TCE.2007.381734).
- [27] C. Ooi and N. Mat Isa, "Quadrants dynamic histogram equalization for contrast enhancement," *IEEE Trans. Consum. Electron.*, vol. 56, no. 4, pp. 2552–2559, Nov. 2010, doi: [10.1109/TCE.2010.5681140](https://doi.org/10.1109/TCE.2010.5681140).
- [28] C.-H. Lu, H.-Y. Hsu, and L. Wang, "A new contrast enhancement technique by adaptively increasing the value of histogram," in *Proc. IEEE Int. Workshop Imag. Syst. Techn.*, May 2009, pp. 407–411, doi: [10.1109/IST.2009.5071676](https://doi.org/10.1109/IST.2009.5071676).
- [29] A. S. Parihar and O. P. Verma, "Contrast enhancement using entropy-based dynamic sub-histogram equalisation," *IET Image Process.*, vol. 10, no. 11, pp. 799–808, Nov. 2016, doi: [10.1049/iet-ipr.2016.0242](https://doi.org/10.1049/iet-ipr.2016.0242).
- [30] Q. Wang and R. Ward, "Fast Image/Video contrast enhancement based on weighted thresholded histogram equalization," *IEEE Trans. Consum. Electron.*, vol. 53, no. 2, pp. 757–764, 2007, doi: [10.1109/TCE.2007.381756](https://doi.org/10.1109/TCE.2007.381756).
- [31] M. Kim and M. Chung, "Recursively separated and weighted histogram equalization for brightness preservation and contrast enhancement," *IEEE Trans. Consum. Electron.*, vol. 54, no. 3, pp. 1389–1397, Aug. 2008, doi: [10.1109/TCE.2008.4637632](https://doi.org/10.1109/TCE.2008.4637632).
- [32] Y.-R. Lai, P.-C. Tsai, C.-Y. Yao, and S.-J. Ruan, "Improved local histogram equalization with gradient-based weighting process for edge preservation," *Multimedia Tools Appl.*, vol. 76, no. 1, pp. 1585–1613, Jan. 2017, doi: [10.1007/s11042-015-3147-7](https://doi.org/10.1007/s11042-015-3147-7).
- [33] A. K. Bhandari, "A logarithmic law based histogram modification scheme for naturalness image contrast enhancement," *J. Ambient Intell. Humanized Comput.*, vol. 11, pp. 1605–1622, Feb. 2020, doi: [10.1007/s12652-019-01258-6](https://doi.org/10.1007/s12652-019-01258-6).
- [34] T. L. Kong and N. A. M. Isa, "Bi-histogram modification method for non-uniform illumination and low-contrast images," *Multimedia Tools Appl.*, vol. 77, no. 7, pp. 8955–8978, Apr. 2018, doi: [10.1007/s11042-017-4789-4](https://doi.org/10.1007/s11042-017-4789-4).
- [35] M. F. Khan, E. Khan, and Z. A. Abbasi, "Weighted average multi segment histogram equalization for brightness preserving contrast enhancement," in *Proc. IEEE Int. Conf. Signal Process., Comput. Control*, Mar. 2012, pp. 1–6, doi: [10.1109/ISPC.2012.6224340](https://doi.org/10.1109/ISPC.2012.6224340).
- [36] B. Saha, "High-speed quantile-based histogram equalisation for brightness preservation and contrast enhancement," *Int. J. Adv. Res. Educ. Technol.*, vol. 2, no. 3, pp. 1–5, 2015.
- [37] F.-C. Cheng and S.-C. Huang, "Efficient histogram modification using bilateral bezier curve for the contrast enhancement," *J. Display Technol.*, vol. 9, no. 1, pp. 44–50, Jan. 2013.
- [38] K. Zuiderveld, *Contrast Limited Adaptive Histogram Equalization*. San Diego, CA, USA: Academic, 1994.
- [39] J.-Y. Kim, L.-S. Kim, and S.-H. Hwang, "An advanced contrast enhancement using partially overlapped sub-block histogram equalization," *IEEE Trans. Circuits Syst. Video Technol.*, vol. 11, no. 4, pp. 475–484, Apr. 2001, doi: [10.1109/76.915354](https://doi.org/10.1109/76.915354).
- [40] F. Lamberti, B. Montrucchio, and A. Sanna, "CMBFHE: A novel contrast enhancement technique based on cascaded multistep binomial filtering histogram equalization," *IEEE Trans. Consum. Electron.*, vol. 52, no. 3, pp. 966–974, Aug. 2006, doi: [10.1109/TCE.2006.1706495](https://doi.org/10.1109/TCE.2006.1706495).
- [41] P. Tao, Y. Pei, M. Celenk, Q. Fu, and A. Wu, "Adaptive image enhancement method using contrast limitation based on multiple layers BOHE," *J. Ambient Intell. Humanized Comput.*, vol. 11, no. 11, pp. 5031–5043, Nov. 2020, doi: [10.1007/s12652-020-01810-9](https://doi.org/10.1007/s12652-020-01810-9).
- [42] J. B. Zimmerman, S. M. Pizer, E. V. Staab, J. R. Perry, W. McCartney, and B. C. Brenton, "An evaluation of the effectiveness of adaptive histogram equalization for contrast enhancement," *IEEE Trans. Med. Imaging*, vol. 7, no. 4, pp. 304–312, Dec. 1988, doi: [10.1109/42.14513](https://doi.org/10.1109/42.14513).
- [43] Z. Xu, X. Liu, and X. Chen, "Fog removal from video sequences using contrast limited adaptive histogram equalization," in *Proc. Int. Conf. Comput. Intell. Softw. Eng.*, Dec. 2009, pp. 3–6, doi: [10.1109/CISE.2009.5366207](https://doi.org/10.1109/CISE.2009.5366207).
- [44] K. Singh and R. Kapoor, "Image enhancement using exposure based sub image histogram equalization," *Pattern Recognit. Lett.*, vol. 36, pp. 10–14, Jan. 2014, doi: [10.1016/j.patrec.2013.08.024](https://doi.org/10.1016/j.patrec.2013.08.024).
- [45] J. R. Tang and N. A. Mat Isa, "Intensity exposure-based bi-histogram equalization for image enhancement," *Turkish J. Elect. Eng. Comput. Sci.*, vol. 24, no. 5, pp. 3564–3585, 2016.
- [46] S. F. Tan and N. A. M. Isa, "Exposure based multi-histogram equalization contrast enhancement for non-uniform illumination images," *IEEE Access*, vol. 7, pp. 70842–70861, 2019, doi: [10.1109/ACCESS.2019.2918557](https://doi.org/10.1109/ACCESS.2019.2918557).
- [47] I. Fister, X. S. Yang, J. Brest, and D. Fister, "A brief review of nature-inspired algorithms for optimization," *Elektroteh. Vestnik/Electrotech. Rev.*, vol. 80, no. 3, pp. 116–122, 2013.
- [48] D. E. Goldberg and J. H. Holland, "Genetic algorithms and machine learning," in *Machine Learning*, vol. 3. Alphen aan den Rijn, The Netherlands: Kluwer, 1988, pp. 59–99.
- [49] D. Dorigo, K. Prze, and F. Glover, *An Introduction to Differential Evolution: New Ideas in Optimization*. London, U.K.: McGraw-Hill, 1999.
- [50] S. Sette and L. Boullart, "Genetic programming: Principles and applications," *Eng. Appl. Artif. Intell.*, vol. 14, no. 6, pp. 727–736, Dec. 2001.
- [51] J. Kennedy and R. Eberhart, "Particle swarm optimization," in *Proc. Int. Conf. Neural Netw.*, vol. 4, Nov./Dec. 1995, pp. 1942–1948.
- [52] D. Karaboga and B. Basturk, "A powerful and efficient algorithm for numerical function optimization: Artificial bee colony (ABC) algorithm," *J. Global Optim.*, vol. 39, no. 3, pp. 459–471, Oct. 2007.
- [53] F. J. Varela and P. Bourgine, *Toward a practice of autonomous systems: Proceedings of the First European Conference on Artificial Life*. Cambridge, MA, USA: MIT Press, 1992.
- [54] X.-S. Yang, "Firefly algorithm, stochastic test functions and design optimisation," *Int. J. Bio-Inspired Comput.*, vol. 2, no. 2, pp. 78–84, 2010.
- [55] E. Cuevas, M. Cienfuegos, D. Zaldívar, and M. Pérez-Cisneros, "A swarm optimization algorithm inspired in the behavior of the social-spider," *Expert Syst. Appl.*, vol. 40, no. 16, pp. 6374–6384, Nov. 2013.
- [56] R. A. Rutenbar, "Simulated annealing algorithms: An overview," *IEEE Circuits Devices Mag.*, vol. 5, no. 1, pp. 19–26, Jan. 1989.
- [57] E. Rashedi, H. Nezamabadi-pour, and S. Saryazdi, "GSA: A gravitational search algorithm," *Inf. Sci.*, vol. 179, no. 13, pp. 2232–2248, Jun. 2009.
- [58] Z. Woo Geem, J. Hoon Kim, and G. V. Loganathan, "A new heuristic optimization algorithm: Harmony search," *Simulation*, vol. 76, no. 2, pp. 60–68, Feb. 2001.
- [59] E. Atashpaz-Gargari and C. Lucas, "Imperialist competitive algorithm: An algorithm for optimization inspired by imperialistic competition," in *Proc. IEEE Congr. Evol. Comput.*, Sep. 2007, pp. 4661–4667.
- [60] S. Mohan and T. R. Mahesh, "Particle swarm optimization based contrast limited enhancement for mammogram images," in *Proc. 7th Int. Conf. Intell. Syst. Control (ISCO)*, Jan. 2013, pp. 384–388, doi: [10.1109/ISCO.2013.6481185](https://doi.org/10.1109/ISCO.2013.6481185).
- [61] K. G. Dhal, M. Sen, and S. Das, "Cuckoo search-based modified bi-histogram equalisation method to enhance the cancerous tissues in mammography images," *Int. J. Med. Eng. Inform.*, vol. 10, no. 2, pp. 164–187, 2018, doi: [10.1504/IJMEL.2018.091209](https://doi.org/10.1504/IJMEL.2018.091209).
- [62] K. G. Dhal, M. Sen, S. Ray, and S. Das, "Multi-thresholded histogram equalization based on parameterless artificial bee colony," in *Incorporating Nature-Inspired Paradigms in Computational Applications*. Hershey, PA, USA: IGI Global, 2018, pp. 108–126.

- [63] K. G. Dhal and S. Das, "Colour retinal images enhancement using modified histogram equalisation methods and firefly algorithm," *Int. J. Biomed. Eng. Technol.*, vol. 28, no. 2, pp. 160–184, 2018.
- [64] H. Singh, A. Kumar, L. K. Balyan, and G. K. Singh, "Swarm intelligence optimized piecewise gamma corrected histogram equalization for dark image enhancement," *Comput. Electr. Eng.*, vol. 70, pp. 462–475, Aug. 2018.
- [65] M. Wan, G. Gu, W. Qian, K. Ren, Q. Chen, and X. Maldague, "Particle swarm optimization-based local entropy weighted histogram equalization for infrared image enhancement," *Infr. Phys. Technol.*, vol. 91, pp. 164–181, Jun. 2018.
- [66] P. C. Sen, M. Hajra, and M. Ghosh, *Image Enhancement Using Differential Evolution Based Whale Optimization Algorithm*, vol. 937. Singapore: Springer, 2020.
- [67] A. K. Bhandari, P. Kandhway, and S. Maurya, "Salp swarm algorithm-based optimally weighted histogram framework for image enhancement," *IEEE Trans. Instrum. Meas.*, vol. 69, no. 9, pp. 6807–6815, Sep. 2020, doi: 10.1109/tim.2020.2976279.
- [68] (2000). *Pasadena-Houses 2000. Computational Vision*. [Online]. Available: [http://www.vision.caltech.edu/image\\_datasets/Pasadena-Houses-2000.tar](http://www.vision.caltech.edu/image_datasets/Pasadena-Houses-2000.tar)
- [69] (1999). *Faces 1999 (Front) Database Computational Vision*. [Online]. Available: [http://www.vision.caltech.edu/image\\_datasets/faces.tar](http://www.vision.caltech.edu/image_datasets/faces.tar)
- [70] (2006). *DIARETDB1, Evaluation Database and Methodology for Diabetic Retinopathy Algorithms, Machine Vision and Pattern Recognition Research Group*. [Online]. Available: [https://www.it.lut.fi/project/imageret/diaretdb1/diaretdb1\\_v\\_1\\_1.zip](https://www.it.lut.fi/project/imageret/diaretdb1/diaretdb1_v_1_1.zip)



**SAMER HAMEED MAJEED** received the B.Eng. degree in computer engineering from the University of Technology, Baghdad, Iraq, in 2005, and the master's degree in computer engineering from Cankaya University, Ankara, Turkey, in 2014. He is currently pursuing the Ph.D. degree in electrical and electronic engineering with the Universiti Sains Malaysia (USM), Penang, Malaysia. From 2014 to 2019, he worked as an Assistant Lecturer at Al Mansour University College, Baghdad. He was a Core Network Manager at Itisaluna Telecom Operator, Baghdad, from 2010 to 2013. He was a Core Network Engineer at Huawei Corporation and other companies from 2005 to 2010. His research interests include image processing, intelligent systems, biomedical engineering, as well as intelligent diagnostic systems and algorithms.



**NOR ASHIDI MAT ISA** (Member, IEEE) received the B.Eng. degree (First Class Hons.) in electrical and electronic engineering from Universiti Sains Malaysia (USM), in 1999, and the Ph.D. degree in electronic engineering (majoring in image processing and artificial neural network). He is currently a Professor and the Deputy Dean (Academic, Career, and International) with the School of Electrical and Electronic Engineering, USM. His research interests include intelligent systems, image processing, neural networks, biomedical engineering, as well as intelligent diagnostic systems and algorithms.

• • •